Electronic Supplementary Information

Efficient synthesis and unit-selective π-extension of π-fused [4.3.3]propellane as chiral building blocks

Kenichi Kato,*[a] Seigo Tanaka,[a] Nobuyoshi Seto,[a] Keisuke Wada,[a] Masayuki Gon,[b] Shixin Fa,[a] Shunsuke Ohtani,[a] Kazuo Tanaka[b] and Tomoki Ogoshi*[a,c]

[a] Department of Synthetic Chemistry and Biological Chemistry, Graduate School of Engineering, Kyoto University, Nishikyo-ku, Kyoto, 615-8510, Japan
E-mail: katok@sbchem.kyoto-u.ac.jp, ogoshi@sbchem.kyoto-u.ac.jp

[b] Department of Polymer Chemistry, Graduate School of Engineering, Kyoto University, Nishikyo-ku, Kyoto, 615-8510, Japan

[c] WPI Nano Life Science Institute, Kanazawa University, Kakuma-machi, Kanazawa, 920-1192, Japan

Contents

1. General Information

Material in Synthesis

All reagents and solvents were of commercial reagent grade and were used without further purification except where noted. Dehydrated stabilizer free tetrahydrofuran (THF, Super plus grade) and dehydrated CH_2Cl_2 (Super^2 grade) were purchased from Kanto Chemical Co., Inc. Super dehydrated toluene, distilled water, and chromatography-grade activated aluminum oxide were purchased from Wako Pure Chemical Industry, Ltd. Anhydrous inhibitor-free 1,2-dimethoxyethane (DME) and tris(dibenzylideneacetone)dipalladium(0) ($Pd_2(dba)_3$) were purchased from Sigma-Aldrich Co. LLC. Thin-layer Chromatography (TLC) analyses were performed on commercial aluminum plates bearing a 0.25 mm layer of Merck Silica gel 60 F254. Preparative silica gel chromatography was performed on Wakosil 60.

Instrumental

^{1}H (500 and 400 MHz) and ^{13}C (151 and 126 MHz) NMR spectra were recorded on JEOL ECZ600R, ECZ500R, and ECS400 spectrometers. Chemical shifts were reported as the delta scale in ppm relative to tetramethylsilane (TMS, δ = 0.00 ppm for both ^{1}H and ^{13}C) as the internal standard.

High Resolution Atmospheric Pressure Chemical Ionization Fourier Transform (HR-APCI-FT) mass spectra were recorded on a Thermo Fisher Scientific LTQ orbitrap XL instrument by using the APCI method in positive ion mode. High Resolution Electrospray Ionization Fourier Transform (HR-ESI-FT) mass spectra were recorded on a Thermo Fisher Scientific EXACTIVE Plus instrument by using the ESI method in positive ion mode.

Ultraviolet/visible (UV/vis) absorption spectra were recorded on a JASCO V-750 spectrophotometer. Fluorescence spectra were measured on a JASCO FP-8550 spectrofluorometer. Absolute fluorescence quantum yields were determined on a Hamamatsu Photonics Quantaurus-QY C11347 absolute PL quantum yield spectrometer. Optical separations were performed on a Japan Analytical Industry LaboACE LC-5060 recycling HPLC apparatus equipped with a DAICEL CHIRALPAK IA (φ = 20 mm, l = 250 mm) column and the separation was confirmed by reinjection. Purity of the obtained fractions was analyzed on a Hitachi Chromaster HPLC instrument equipped with a DAICEL CHIRALPAK IA (φ = 4.6 mm, l = 250 mm) column. Circular dichroism (CD) spectra were recorded on a JASCO J-1500 circular dichroism spectrometer. Circularly polarized luminescence (CPL) spectra were recorded on a JASCO CPL-200 spectrometer.

All calculations were carried out using the *Gaussian 16* program.[S1] The structure was fully optimized without any symmetry restriction. The calculations were performed by the density functional theory (DFT) method with RB3LYP level,[S2] employing a basis set 6-31G(d). After the optimization, electronic states and transitions were computed with TD-SCF/RϖB97X-D level,[S3] employing a basis set 6-31+G(d,p).

2. Synthetic Procedures and Compound Data

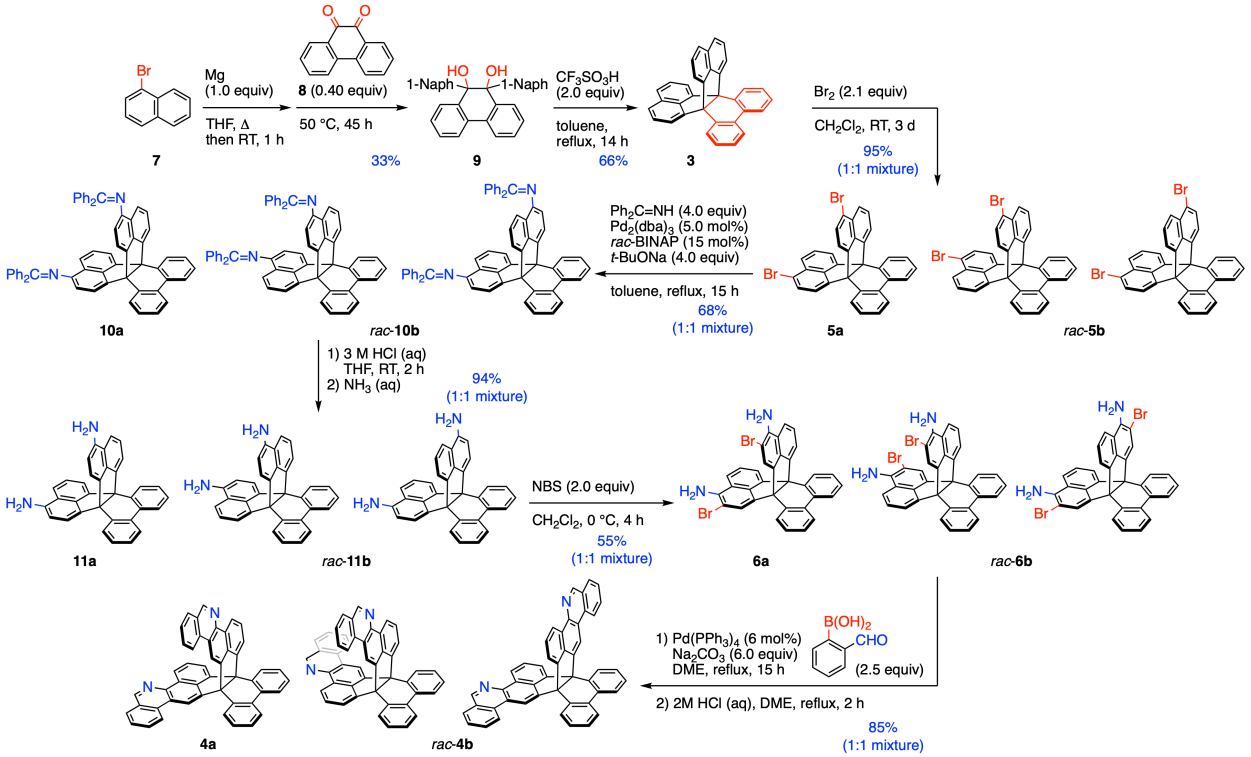

Scheme S2-1. Synthetic route to π-extended [4.3.3]propellanes. 1-Naph = 1-naphthyl, $Pd_2(dba)_3$ = tris(dibenzylideneacetone)dipalladium(0), BINAP = 2,2'-bis(diphenylphosphino)-1,1'-binaphthyl, NBS = *N*-bromosuccinimide, DME = 1,2-dimethoxyethane.

9,10-Di(naphthalen-1-yl)-9,10-dihydrophenanthrene-9,10-diol (9): To magnesium turnings (2.43 g. 100 mmol) placed in a 500-mL round-bottom flask, THF (200 mL) and a few shots of iodine were added under nitrogen atmosphere. To the stirred mixture, 1-bromonaphthalene (**7**, 14.0 mL, 100 mmol) was slowly introduced, and the mixture was stirred at room temperature for 1 h. 9,10-Phenanthrenequinone (**8**, 8.33 g, 40.0 mmol) was added to the resulting suspension. After stirring at 50 °C for 45 h, the mixture was quenched with dilute HCl (aq). The mixture was extracted with EtOAc three times. The organic extract was washed with $NaHCO_3$ (aq) and NaCl (aq) and was passed through a short column of anhydrous Na_2SO_4 and silica gel. After the solvent was evaporated under reduced pressure, purification by column chromatography on Wakosil 60 (toluene) and the subsequent recrystallization (CH_2Cl_2/*n*-hexane) afforded **9** (6.01 g, 13.0 mmol, 33%) as off-white solid. ^{1}H NMR (500 MHz, $CDCl_3$, 298 K): δ / ppm = 9.91 (s, broad, 1H,), 8.30 (s, broad, 1H), 7.99 (s, broad, 1H), 7.82 (d, J = 9.5 Hz, 2H), 7.78–7.63 (m, 4H), 7.54–7.32 (m, 5H), 7.23–6.94 (m, 8H), 2.29 (s, broad, 1H, O<u>H</u>), and 2.10 (s, broad, 1H, O<u>H</u>); ^{13}C NMR (126 MHz, acetone-d_6, 298 K): δ / ppm = 141.40, 140.35, 135.07, 134.42, 133.19, 132.34, 131.40, 130.44, 129.22, 128.91, 128.59, 128.37, 124.93, 124.48, 124.37, 123.40, and 82.09; HR ESI-FT-MS (positive): m/z calcd for $[C_{34}H_{24}O_2Na]^+$: 487.1649 $[M+Na]^+$; found: 487.1669.

[4.3.3]Propellane 3: 9,10-Di(naphthalen-1-yl)-9,10-dihydrophenanthrene-9,10-diol (**3**, 6.20 g, 13.3 mmol) was suspended in toluene (267 mL) in a 500-mL round-bottom flask under nitrogen atmosphere. The mixture was warmed up to 90 °C and trifluoromethanesulfonic acid (2.36 mL, 26.6 mmol) was slowly introduced to the flask. The mixture was refluxed for 14 h before the reaction was quenched with ice and water. The mixture was extracted with $CHCl_3$ three times. The organic extract was passed through a short column of silica gel. After the solvent was evaporated under reduced pressure, recrystallization (CH_2Cl_2/*n*-hexane) afforded **3** (3.77 g, 8.79 mmol, 66%) as off-white solid. ^{1}H NMR (400 MHz, $CDCl_3$, 298 K): δ / ppm = 8.34 (d, J = 8.0 Hz, 2H), 7.95 (d, J = 7.6 Hz, 2H), 7.65 (d, J = 6.8 Hz, 4H), 7.56 (d, J = 8.0 Hz, 4H), 7.49–7.41 (m, 6H), and 7.32 (t, J = 7.6 Hz, 2H); ^{13}C NMR (126 MHz, acetone-d_6, 298 K): δ / ppm = 149.10, 137.05, 136.95, 132.55, 131.97, 130.03, 129.09, 128.94, 128.44, 124.74, 124.49, 121.71, and 68.40; HR APCI-TOF-MS (positive): m/z calcd for $[C_{34}H_{21}]^+$: 429.1638 $[M+H]^+$; found: 429.1638.

Dibromo[4.3.3]propellanes 5a and *rac*-5b: [4.3.3]Propellane **3** (2.02 g, 4.71 mmol) was dissolved in CH_2Cl_2 (118 mL) in a 200-mL round-bottom flask under nitrogen atmosphere. To the solution, bromine (0.51 mL, 9.9 mmol) was slowly introduced. The mixture was stirred at room temperature for 3 d before the reaction was quenched with $Na_2S_2O_3$ (aq). The mixture was extracted with $CHCl_3$ three times. The organic extract was passed through a short column of anhydrous Na_2SO_4 and silica gel. Evaporation of the solvent under reduced pressure afforded a mixture of **5a** and *rac*-**5b** (2.64 g, 4.50 mmol, 95%) as off-white solid. ^{1}H NMR (500 MHz, $CDCl_3$, 298 K): δ / ppm = 8.25–8.19 (m, 2H), 7.95 (d, J = 7.5 Hz, 2H), 7.77 (d, J = 8.0 Hz, 2H), 7.71–7.67 (m, 4H), 7.60–7.57 (m, 2H), 7.49–7.46 (m, 2H), 7.45–7.41 (m, 2H), and 7.34 (t, J = 7.8 Hz, 2H); ^{13}C NMR (126 MHz, $CDCl_3$, 298 K): δ / ppm = 147.87, 147.75, 147.55, 147.45, 137.18, 135.09, 135.02, 134.93, 131.27, 131.23, 131.21, 131.08, 130.95, 129.22, 128.62, 128.57, 128.51, 128.23, 127.74, 124.17, 123.45, 123.43, 121.63, 121.54, 121.47, 121.39, 118.71, 67.76, 67.18, and 66.61; HR APCI-FT-MS (positive): m/z calcd for $[C_{34}H_{19}{}^{79}Br_2]^+$: 584.9848 $[M+H]^+$; found: 584.9846.

Bis[(diphenylmethylene)amino][4.3.3]propellanes 10a and *rac*-10b: A mixture of [4.3.3]propellane **5a** and *rac*-**5b** (1.17 g, 2.00 mmol), tris(dibenzylideneacetone)dipalladium(0) ($Pd_2(dba)_3$, 94 mg, 5.0 mol%), *rac*-2,2'-bis(diphenylphosphino)-1,1'-binaphthyl (*rac*-BINAP, 186 mg, 15 mol%), and sodium *tert*-butoxide (*t*-BuONa, 768 mg, 8.00 mmol) were dissolved in toluene (200 mL) in a 500-mL round-bottom flask under nitrogen atmosphere. To the solution, benzophenoneimine (1.34 mL, 8.00 mmol) was added and the mixture was refluxed for 15 h. The reaction was quenched with $Na_2S_2O_3$ (aq). The mixture was passed through a short column of Celite using CH_2Cl_2 and acetone as eluent. After the solvent was evaporated under reduced pressure, purification by column chromatography on Wakosil 60 (CH_2Cl_2/*n*-hexane = 1/3 to 1/0) afforded a mixture of **10a** and *rac*-**10b** (1.04 g, 1.36 mmol, 68%) as yellow solid. ^{1}H NMR (400 MHz, acetone-d_6, 298 K) for **10a**: δ / ppm = 8.57 (dd, J = 7.8, 1.0 Hz, 1H, biphenyl-H), 8.37 (dd, J = 7.8, 1.0 Hz, 1H, biphenyl-H), 8.07–8.02 (m, 2H, biphenyl-H), 7.85 (d, J = 7.2 Hz, 2H), 7.77–7.75 (m, 4H), 7.69 (d, J = 8.0 Hz, 2H), 7.53–7.43 (m, 12H), 7.42–7.28 (m, 2H), 7.18–7.07 (m, 10H), and 6.60 (d, J = 7.6 Hz, 2H, Naph-H next to imine); ^{1}H NMR (400 MHz, acetone-

d_6, 298 K) for **10b**: δ / ppm = 8.46 (dd, J = 7.8, 1.0 Hz, 2H, biphenyl-H), 8.03 (dd, J = 7.8, 1.0 Hz, 2H, biphenyl-H), 7.80–7.75 (m, 6H), 7.68 (d, J = 8.0 Hz, 2H), 7.59–7.43 (m, 12H), 7.42–7.28 (t, J = 7.8 Hz, 2H), 7.18–7.07 (m, 10H), and 6.56 (d, J = 7.2 Hz, 2H, Naph-H next to imine); ^{13}C NMR (126 MHz, acetone-d_6, 298 K): δ / ppm = 169.24, 149.57, 149.08, 146.30, 146.18, 144.47, 143.96, 140.32, 137.64, 137.56, 137.44, 137.31, 137.24, 131.97, 131.80, 131.73, 131.67, 130.59, 130.02, 129.95, 129.47, 129.42, 129.29, 129.12, 129.06, 128.98, 128.82, 128.42, 128.38, 128.31, 128.21, 126.61, 124.66, 124.62, 124.55, 122.31, 122.01, 121.43, 121.32, 121.28, 121.02, 117.31, 117.28, 68.95, 68.07, and 67.20; HR APCI-FT-MS (positive): m/z calcd for $[C_{60}H_{39}N_2]^+$: 787.3108 $[M+H]^+$; found: 787.3107.

Diamino[4.3.3]propellanes 11a and *rac*-11b: A mixture of [4.3.3]propellane **10a** and *rac*-**10b** (787 mg, 1.00 mmol) was dissolved in THF (60 mL) in a 200-mL round-bottom flask. To the solution, aqueous HCl solution (3 M, 60 mL) was added, and the mixture was stirred at room temperature for 2 h. The reaction was quenched with aqueous NH_3 solution (25%). The mixture was extracted with $CHCl_3$ three times. The organic extract was passed through a short column of anhydrous Na_2SO_4. After the solvent was evaporated under reduced pressure, purification by column chromatography on Wakosil 60 (CH_2Cl_2/acetone = 1/0 to 10/1) afforded a mixture of **11a** and *rac*-**11b** (430 mg, 0.937 mmol, 94%) as purple solid. ^{1}H NMR (400 MHz, $CDCl_3$, 298 K): δ / ppm = 8.32–8.24 (m, 2H), 7.95–7.90 (m, 2H), 7.64–7.52 (m, 2H), 7.48–7.37 (m, 8H), 7.35–7.27 (m, 2H), 6.73–6.67 (m, 2H), and 4.00 (s, 4H, N<u>H</u>$_2$); ^{13}C NMR (151 MHz, acetone-d_6, 298 K): δ / ppm = 170.81, 149.78, 149.62, 149.58, 149.42, 149.38, 149.19, 149.00, 146.60, 146.50, 146.25, 144.41, 144.19, 143.99, 143.73, 143.10, 143.02, 142.73, 138.93, 138.41, 138.32, 138.25, 138.21, 138.14, 137.96, 137.90, 137.86, 137.80, 137.75, 137.59, 137.44, 137.29, 132.25, 132.07, 131.92, 131.85, 131.76, 131.70, 130.08, 129.12, 129.10, 129.07, 128.94, 128.92, 128.74, 128.40, 128.32, 128.25, 128.22, 128.18, 128.11, 128.06, 127.99, 127.93, 127.74, 126.81, 126.77, 126.73, 126.64, 125.12, 125.09, 125.05, 124.70, 124.66, 124.63, 124.59, 124.54, 124.51, 124.45, 124.39, 122.67, 122.63, 122.60, 122.44, 122.41, 122.20, 121.87, 121.79, 121.72, 121.43, 121.31, 121.28, 121.22, 121.10, 121.00, 120.92, 120.86, 120.68, 119.85, 119.75, 119.68, 119.44, 116.48, 116.41, 116.23, 110.42, 110.39, 110.36, 110.21, 68.96, 68.91, 68.09, 68.04, 67.70, 67.22, 66.82, 55.48, 55.45, and 54.98; HR APCI-FT-MS (positive): m/z calcd for $[C_{34}H_{23}N_2]^+$: 459.1856 $[M+H]^+$; found: 459.1857.

Dibromodiamino[4.3.3]propellanes 6a and *rac*-6b: *N*-Bromosuccinimide (72 mg, 0.40 mmol) was dissolved in CH_2Cl_2 (2.5 mL) in a 50-mL round-bottom flask under nitrogen atmosphere. After the mixture was cooled down to 0 °C, [4.3.3]propellane **11a** and *rac*-**11b** (92 mg, 0.20 mmol) was added to the flask. The mixture was stirred at 0 °C for 4 h before the reaction was quenched with $NaHCO_3$ (aq). The mixture was extracted with CH_2Cl_2 three times. The organic extracts were dried over anhydrous Na_2SO_4, and the solvent was evaporated under reduced pressure. Purification by column chromatography on Wakosil 60 (CH_2Cl_2/*n*-hexane = 3/1) afforded a mixture of **6a** and *rac*-**6b** (67 mg, 0.11 mmol, 55%) as peach solid. ^{1}H NMR (400 MHz, $CDCl_3$, 298 K): δ / ppm = 8.21–8.15 (m, 2H), 7.94 (d, J = 8.0 Hz, 2H), 7.64–7.57 (m, 4H), 7.49–7.38 (m, 6H), and 7.34–7.29 (m, 2H); ^{13}C NMR (151 MHz, acetone-d_6, 298 K): δ / ppm = 149.18, 149.01, 140.02, 139.98, 139.91, 139.87, 138.68, 138.52, 137.42, 137.04, 137.03, 136.66, 132.14, 131.89, 131.62, 129.98, 129.28, 129.14, 128.99, 128.47, 128.41, 128.33,

128.22, 128.09, 125.82, 125.77, 124.78, 124.73, 124.66, 122.36, 122.17, 122.10, 120.05, 119.92, 104.54, 104.50, 104.36, 104.32, 68.74, 67.49, and 66.29; HR APCI-FT-MS (positive) *m*/*z* calcd for $[C_{34}H_{21}N_2{}^{79}Br_2]^+$: 615.0066 $[M+H]^+$; found: 615.0067.

General procedure for π-extension of dibromodiamino[4.3.3]propellanes: A mixture of [4.3.3]propellane **6a** and *rac*-**6b** (45 mg, 0.075 mmol), (2-formylphenyl)boronic acid (28 mg, 0.18 mmol), and tetrakis(triphenylphosphine)palladium(0) ($Pd(PPh_3)_4$, 6 mg, 6 mol%) were dissolved in DME (3.8 mL) in a round-bottom flask under nitrogen atmosphere. To the mixture, a degassed solution of Na_2CO_3 (48 mg, 0.45 mmol) in distilled water (2.3 mL) was added, and the mixture was refluxed for 15 h. After the mixture was cooled down to room temperature, aqueous HCl solution (2 M, 1.5 mL) was added. The mixture was refluxed for 2 h and was quenched with $NaHCO_3$ (aq). The mixture was extracted with $CHCl_3$ three times. The organic extract was passed through a short column of anhydrous Na_2SO_4 and activated Al_2O_3, and the solvent was evaporated under reduced pressure. Purification by column chromatography on Wakosil 60 (CH_2Cl_2/*n*-hexane = 1/1 to 1/0, then CH_2Cl_2/acetone = 50/1 to 10/1) afforded a mixture of **4a** and *rac*-**4b** (40 mg, 0.063 mmol, 85%) as orange solid. The mixture was further separated into **4a**, (*R*,*R*)-**4b**, and (*S*,*S*)-**4b**, using HPLC apparatus equipped with a chiral column.

Compound data for 4a: ^{1}H NMR (400 MHz, $CDCl_3$, 298 K): δ / ppm = 9.38 (s, 2H), 8.83 (d, *J* = 8.0 Hz, 2H), 8.78 (d, *J* = 8.4 Hz, 2H), 8.75 (s, 2H), 8.56 (d, *J* = 8.0 Hz, 1H, biphenyl-H), 8.37 (d, *J* = 7.6 Hz, 1H, biphenyl-H), 8.11 (d, *J* = 8.0 Hz, 2H), 8.04 (d, *J* = 8.0 Hz, 1H, biphenyl-H), 8.01 (d, *J* = 8.0 Hz, 1H, biphenyl-H), 7.93–7.87 (m, 4H), 7.79 (t, *J* = 7.8 Hz, 2H), 7.72 (t, *J* = 7.6 Hz, 2H), 7.54 (t, *J* = 7.6 Hz, 1H, biphenyl-H), 7.48 (t, *J* = 7.6 Hz, 1H, biphenyl-H), 7.41 (t, *J* = 7.6 Hz, 1H, biphenyl-H), and 7.36 (t, *J* = 7.6 Hz, 1H, biphenyl-H); ^{13}C NMR (126 MHz, $CDCl_3$, 298 K): δ / ppm = 151.62, 147.21, 147.19, 140.48, 136.65, 135.64, 135.00, 133.23, 131.93, 131.29, 130.65, 130.38, 129.10, 128.97, 128.81, 128.34, 128.25, 127.86, 127.64, 127.17, 126.90, 124.50, 124.20, 123.41, 122.59, 122.55, 121.99, 114.71, 68.61, and 67.75; HR APCI-FT-MS (positive): *m*/*z* calcd for $[C_{48}H_{27}N_2]^+$: 631.2169 $[M+H]^+$; found: 631.2170; UV/vis ($CHCl_3$): λ_{max} / nm (ε / M^{-1} cm^{-1}) = 265 (1.6×10^5), 336 (2.8×10^4), 351 (2.8×10^4), and 368 (2.7×10^4); FL ($CHCl_3$, 5.3×10^{-6} M, Φ_{FL} = 0.36): λ_{max} / nm = 373, 393, and 414.

Compound data for 4b: ^{1}H NMR (400 MHz, $CDCl_3$, 298 K): δ / ppm = 9.39 (s, 2H), 8.83 (d, *J* = 8.4 Hz, 2H), 8.79 (d, *J* = 9.6 Hz, 2H), 8.74 (s, 2H), 8.50 (d, *J* = 6.8 Hz, 2H, biphenyl-H), 8.13 (d, *J* = 8.0 Hz, 2H), 8.03 (d, *J* = 7.2 Hz, 2H, biphenyl-H), 7.98–7.92 (m, 4H), 7.78–7.72 (m, 4H), 7.55 (t, *J* = 7.6 Hz, 2H, biphenyl-H), 7.40 (t, *J* = 7.0 Hz, 2H, biphenyl-H); ^{13}C NMR (126 MHz, $CDCl_3$, 298 K): δ / ppm = 151.59, 147.59, 146.92, 140.44, 136.62, 135.42, 133.26, 131.59, 130.73, 130.40, 128.90, 128.87, 128.81, 128.34, 127.74, 127.23, 126.91, 124.37, 123.56, 123.19, 122.56, 122.09, 114.03, and 68.08; HR APCI-FT-MS (positive): *m*/*z* calcd for $[C_{48}H_{27}N_2]^+$: 631.2169 $[M+H]^+$; found: 631.2170; UV/vis ($CHCl_3$): λ_{max} / nm (ε / M^{-1} cm^{-1}) = 268 (1.4×10^5), 351 (3.1×10^4), 336 (2.9×10^4), and 369 (3.2×10^4); FL ($CHCl_3$, 5.8×10^{-6} M, Φ_{FL} = 0.36): λ_{max} / nm = 373, 392, and 414; 1st fraction (>99%ee): CD ($CHCl_3$): λ_{max} / nm ($\Delta\varepsilon$ / M^{-1} cm^{-1}, g_{CD}) = 286 (135, 2.3×10^{-3}), 320 (47, 2.3×10^{-3}), 352 (36, 1.2×10^{-3}), and 368 (27, 0.8×10^{-3}); CPL ($CHCl_3$):

λ_{max} / nm (g_{CPL}) = ca. 380 (6.5×10^{-4}); 3rd fraction (>99%ee): CD ($CHCl_3$): λ_{max} / nm ($\Delta\varepsilon$ / M^{-1} cm^{-1}, g_{CD}) = 286 (–141, -2.5×10^{-3}), 320 (–52, -2.6×10^{-3}), 352 (–43, -1.4×10^{-3}), and 368 (–39, -1.2×10^{-3}); CPL ($CHCl_3$): λ_{max} / nm (g_{CPL}) = ca. 380 (-7.1×10^{-4}).

3. ^{1}H and ^{13}C NMR Spectra

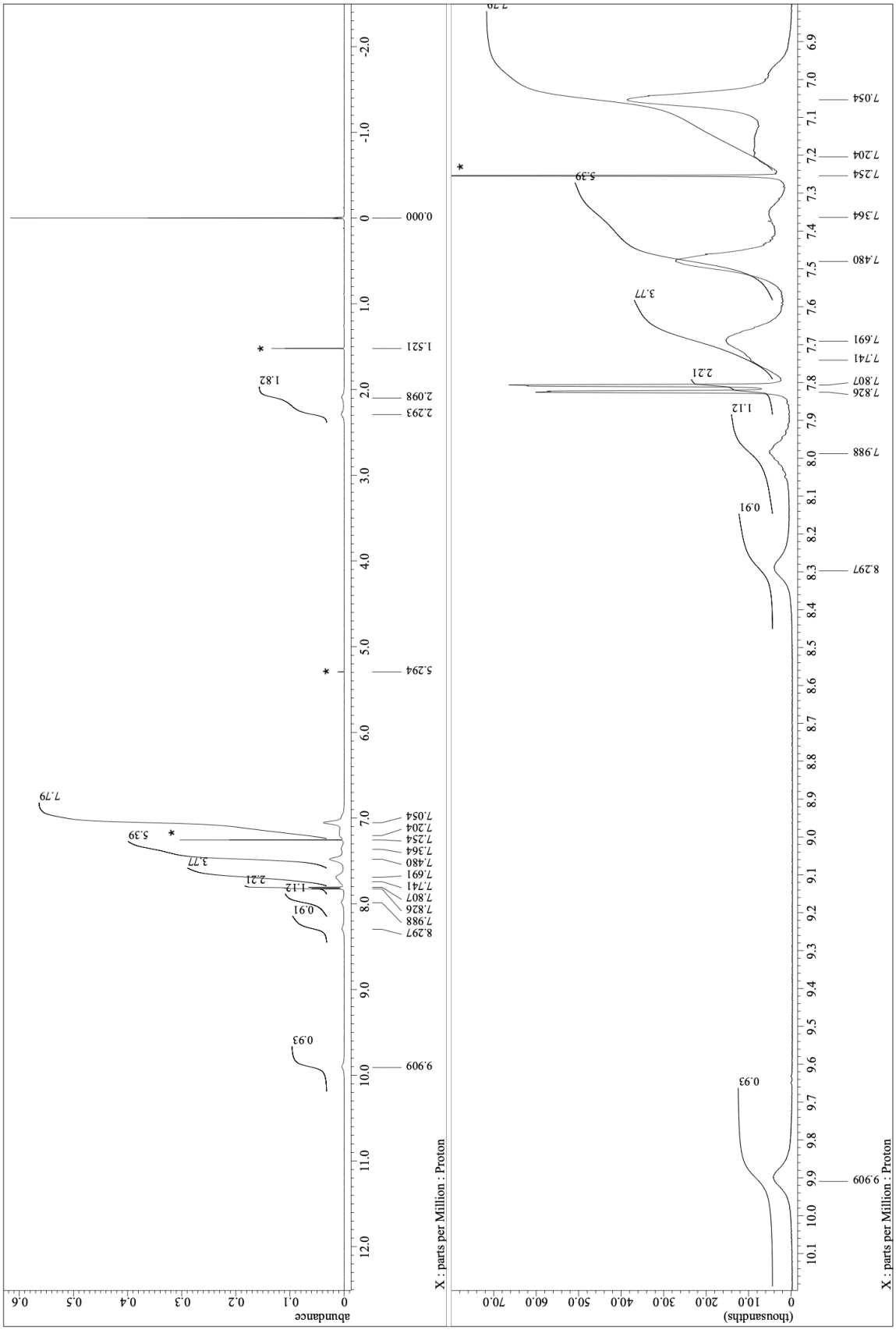

Figure S3-1. ^{1}H (500 MHz) NMR spectrum of **9** in $CDCl_3$ at room temperature. Peaks marked with * are due to residual solvents.

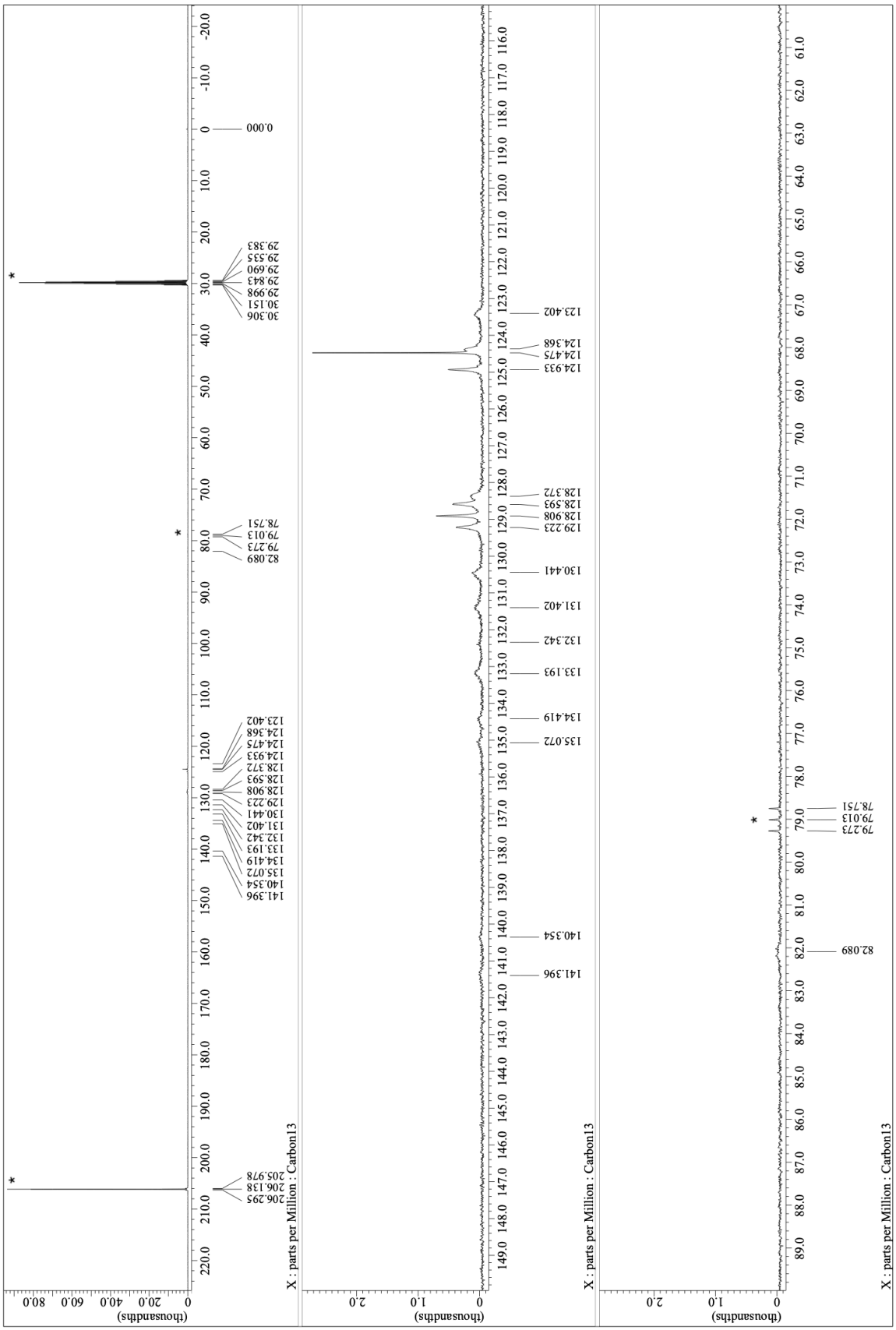

Figure S3-2. ^{13}C (126 MHz) NMR spectrum of **9** in acetone-d_6 at room temperature. Peaks marked with * are due to residual solvents.

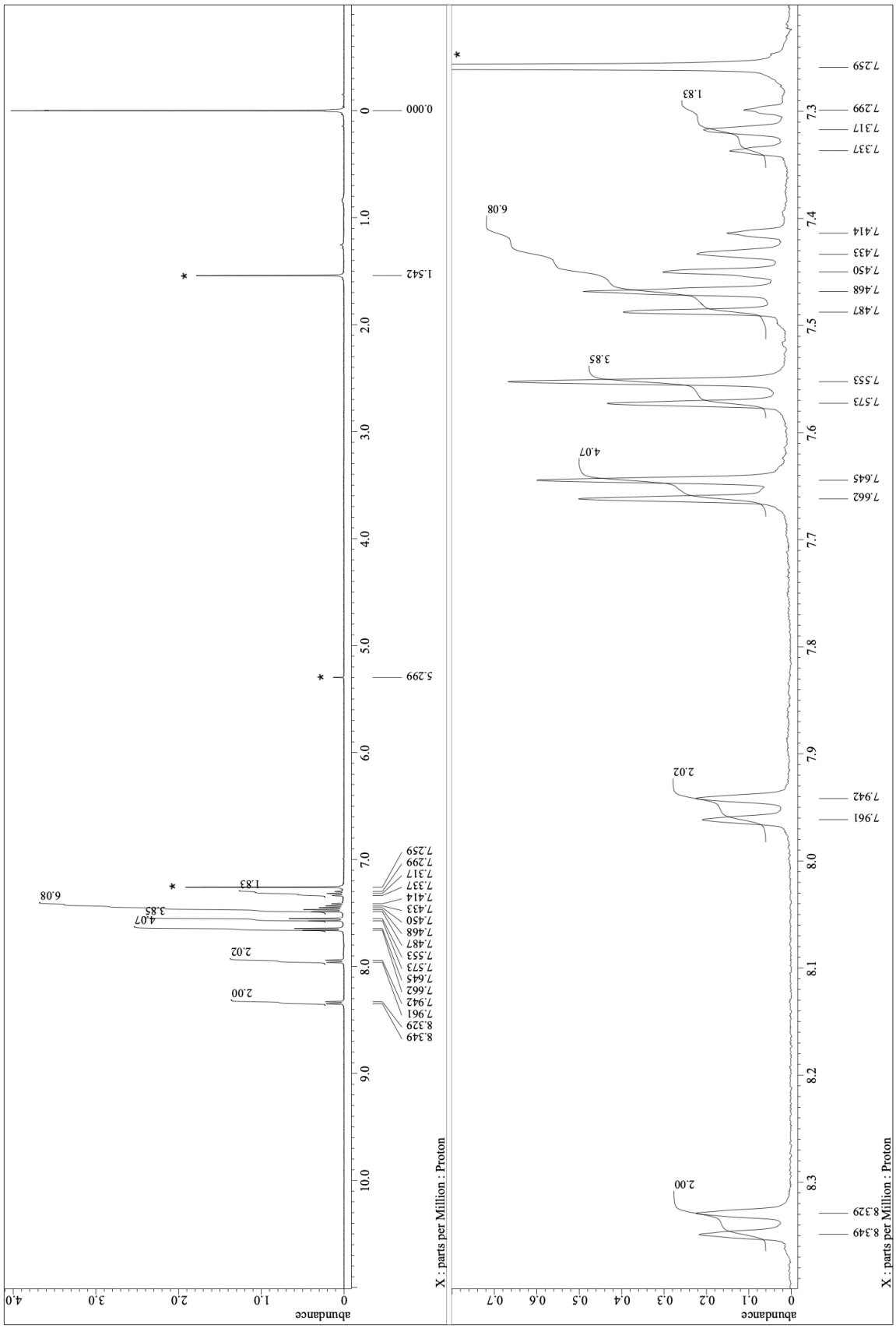

Figure S3-3. ^{1}H (400 MHz) NMR spectrum of **3** in $CDCl_3$ at room temperature. Peaks marked with * are due to residual solvents.

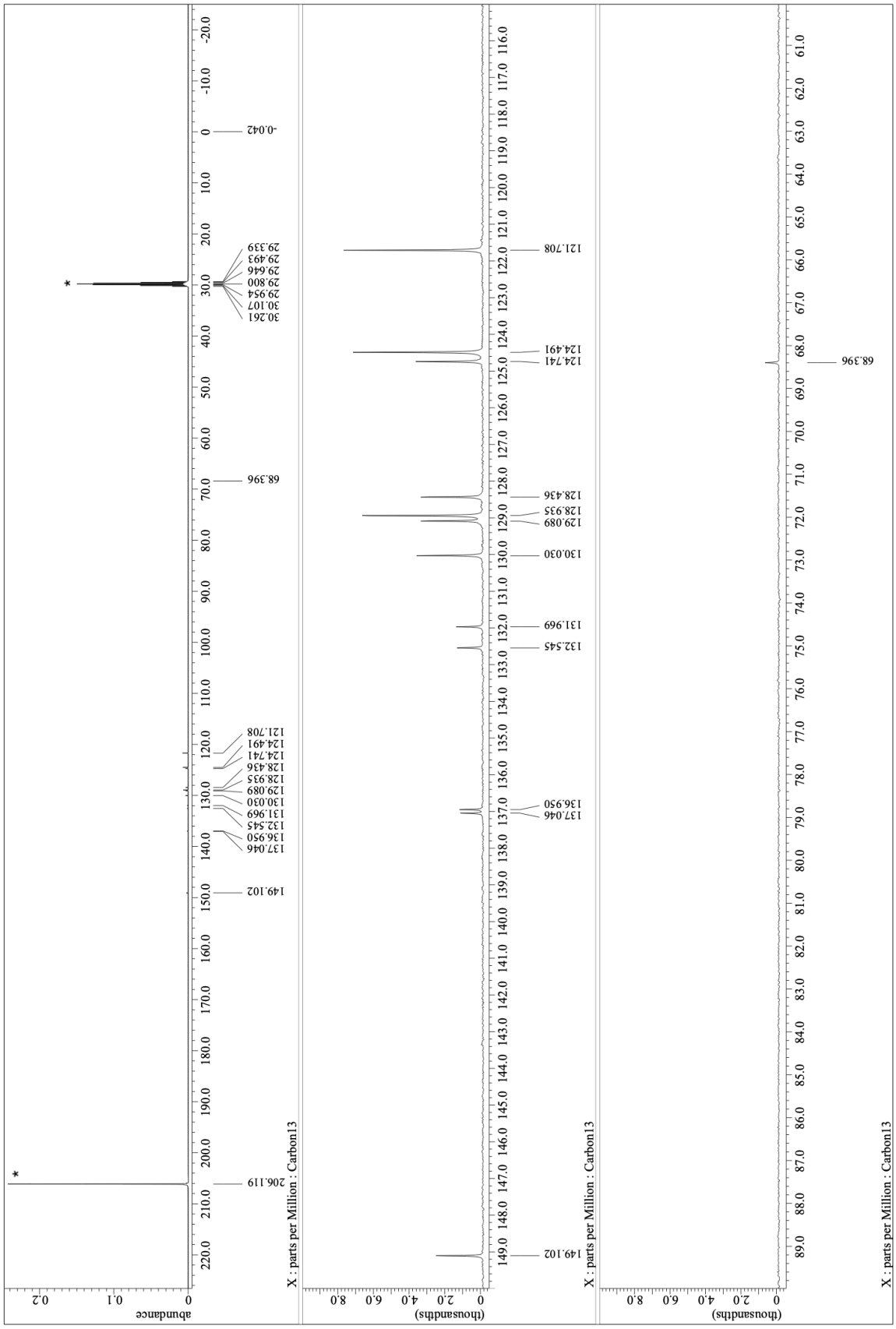

Figure S3-4. ^{13}C (126 MHz) NMR spectrum of **3** in acetone-d_6 at room temperature. Peaks marked with * are due to residual solvents.

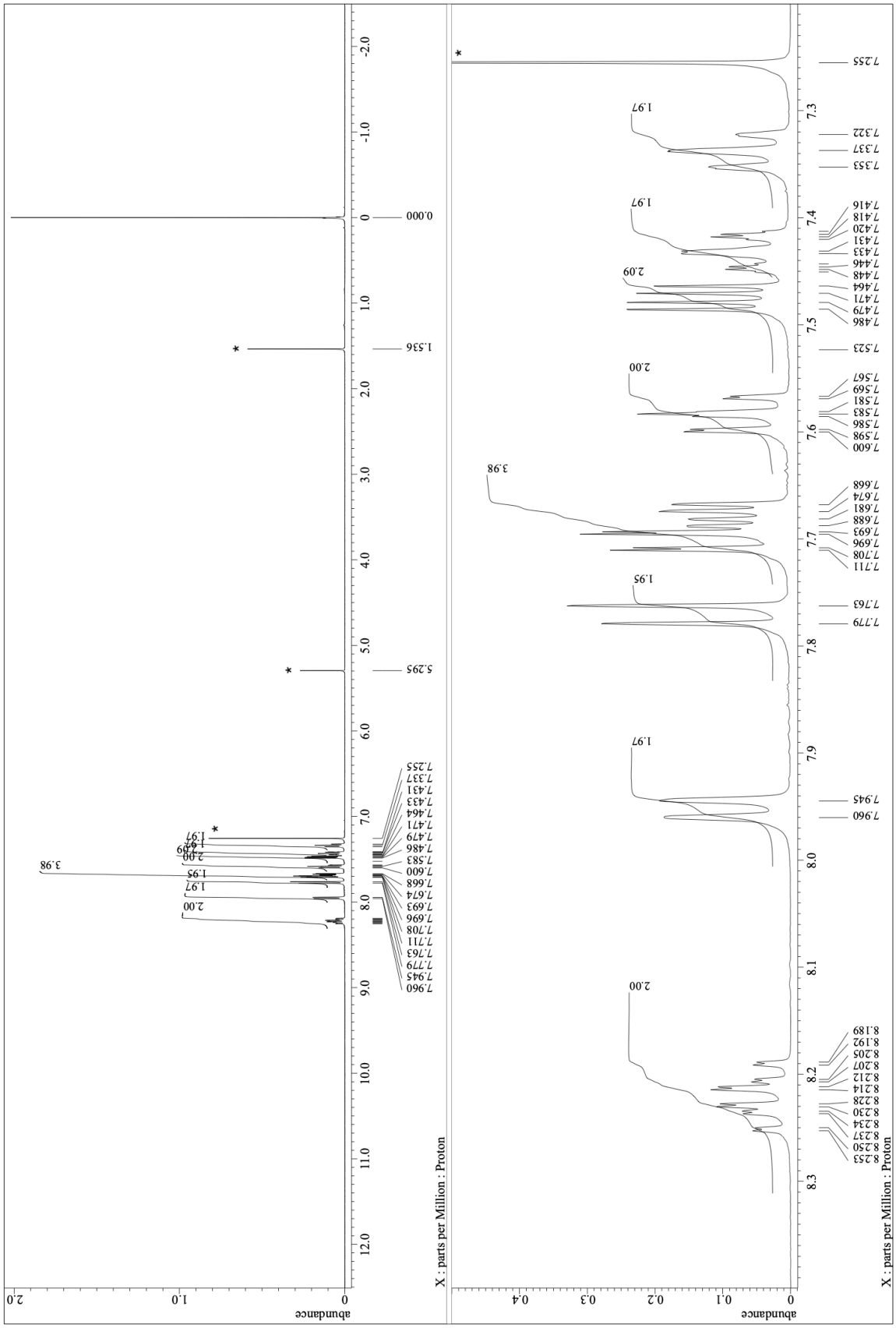

Figure S3-5. ^{1}H (500 MHz) NMR spectra of **5a**,**b** in $CDCl_3$ at room temperature. Peaks marked with * are due to residual solvents.

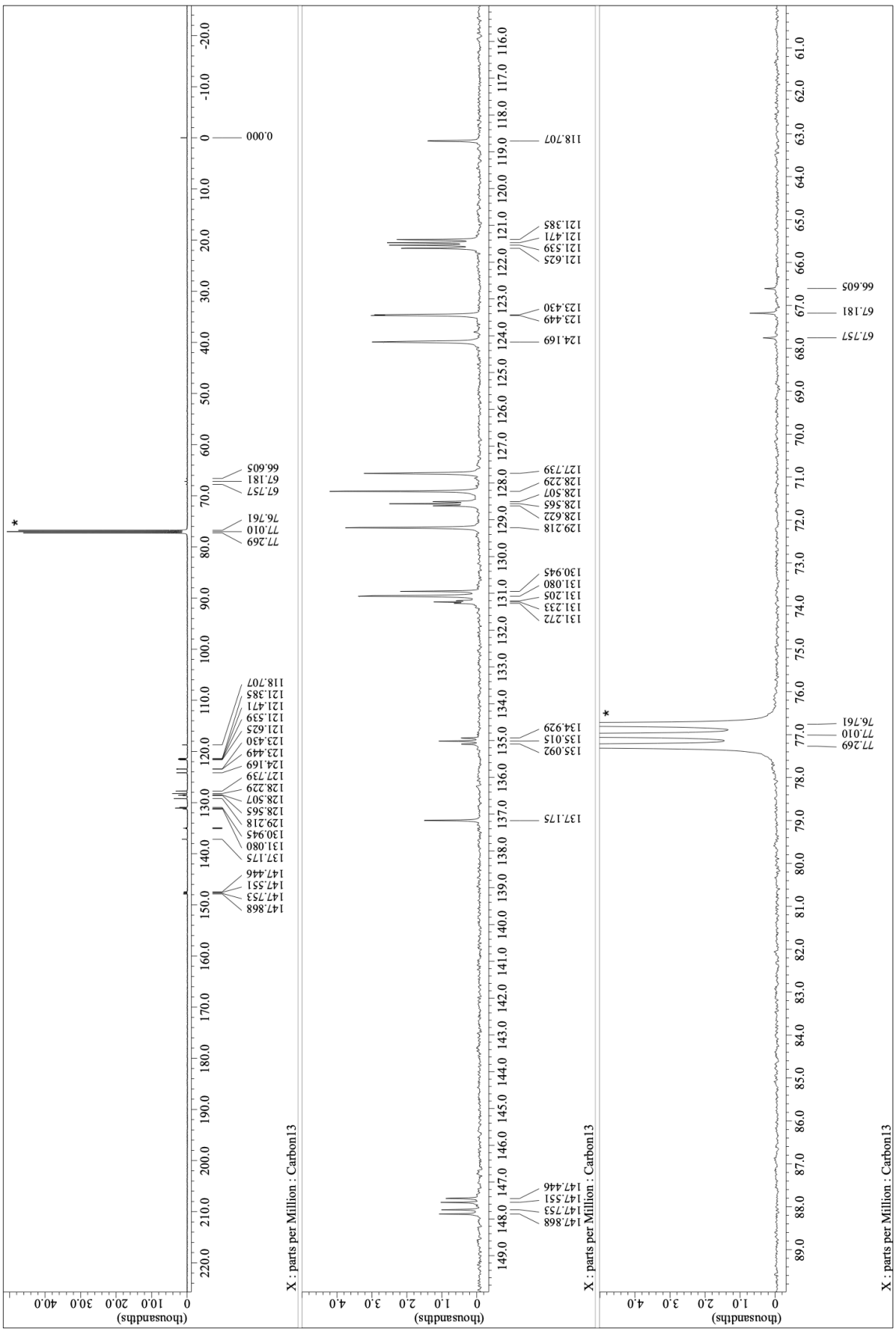

Figure S3-6. ^{13}C (126 MHz) NMR spectra of **5a**,**b** in $CDCl_3$ at room temperature. Peaks marked with * are due to residual solvents.

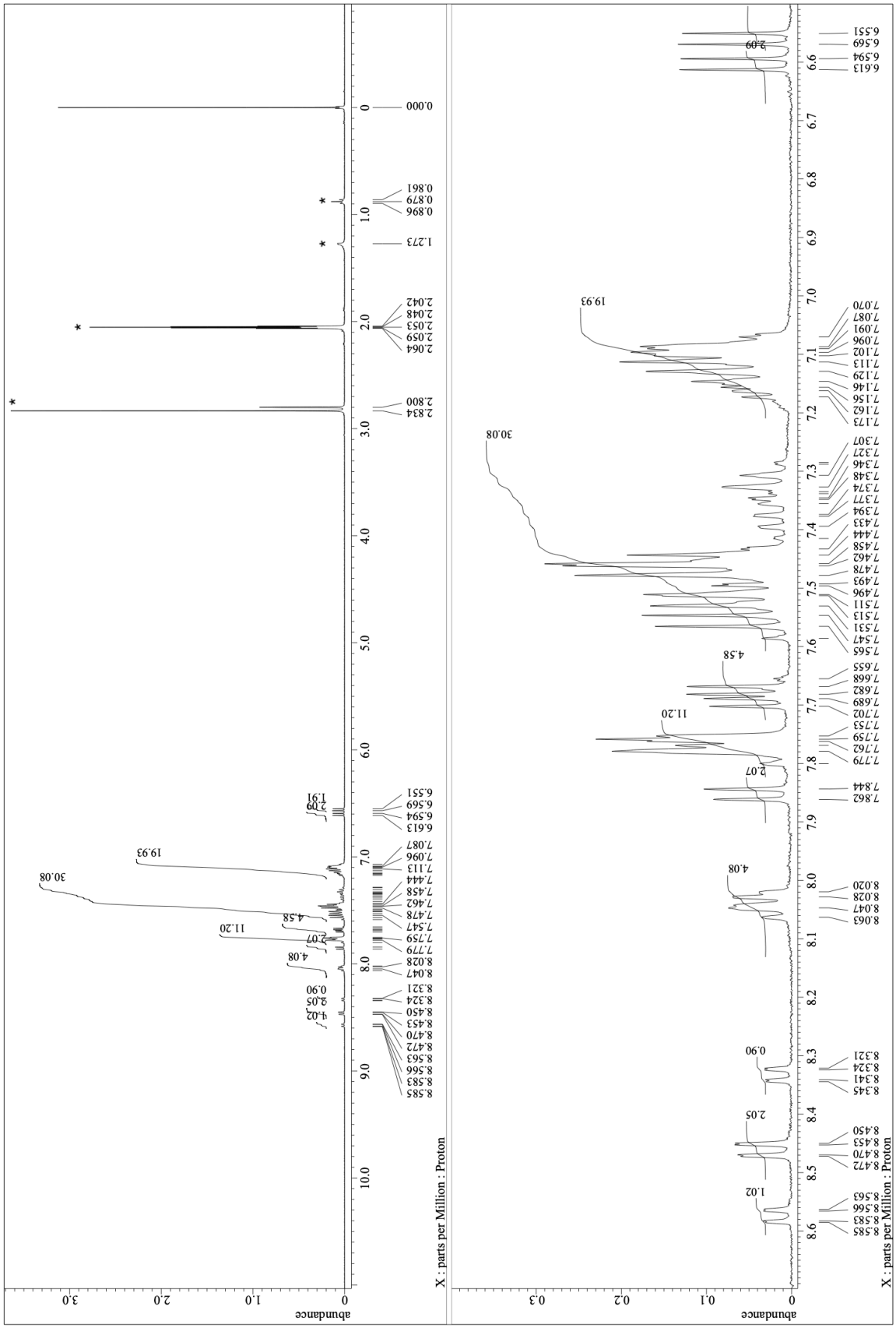

Figure S3-7. ^{1}H (400 MHz) spectra of **10a**,**b** in acetone-d_6 at room temperature. Peaks marked with * are due to residual solvents.

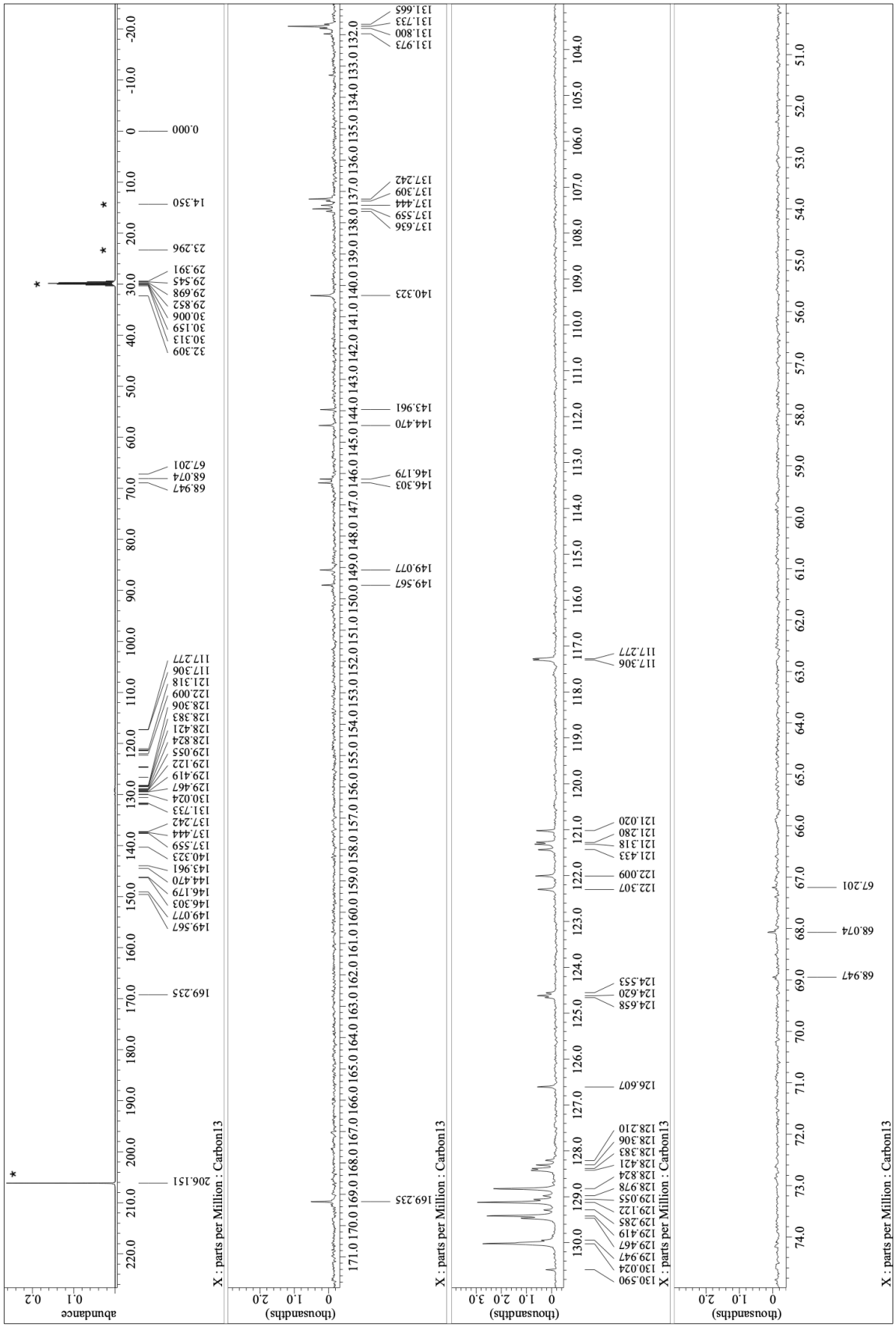

Figure S3-8. ^{13}C NMR (126 MHz) spectra of **10a**,**b** in acetone-d_6 at room temperature. Peaks marked with * are due to residual solvents.

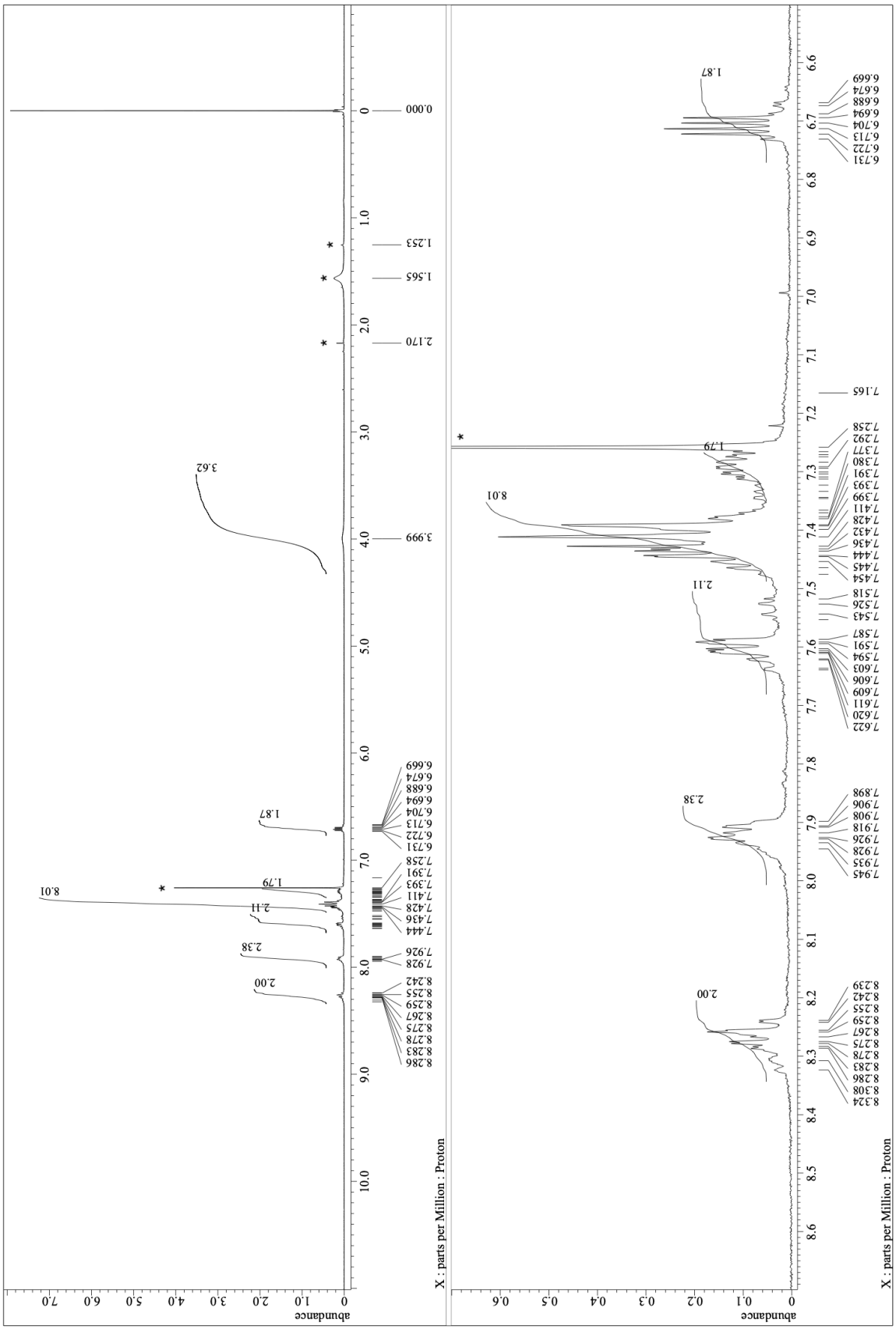

Figure S3-9. ^{1}H (400 MHz) NMR spectrum of **11a,b** in $CDCl_3$ at room temperature. Peaks marked with * are due to residual solvents.

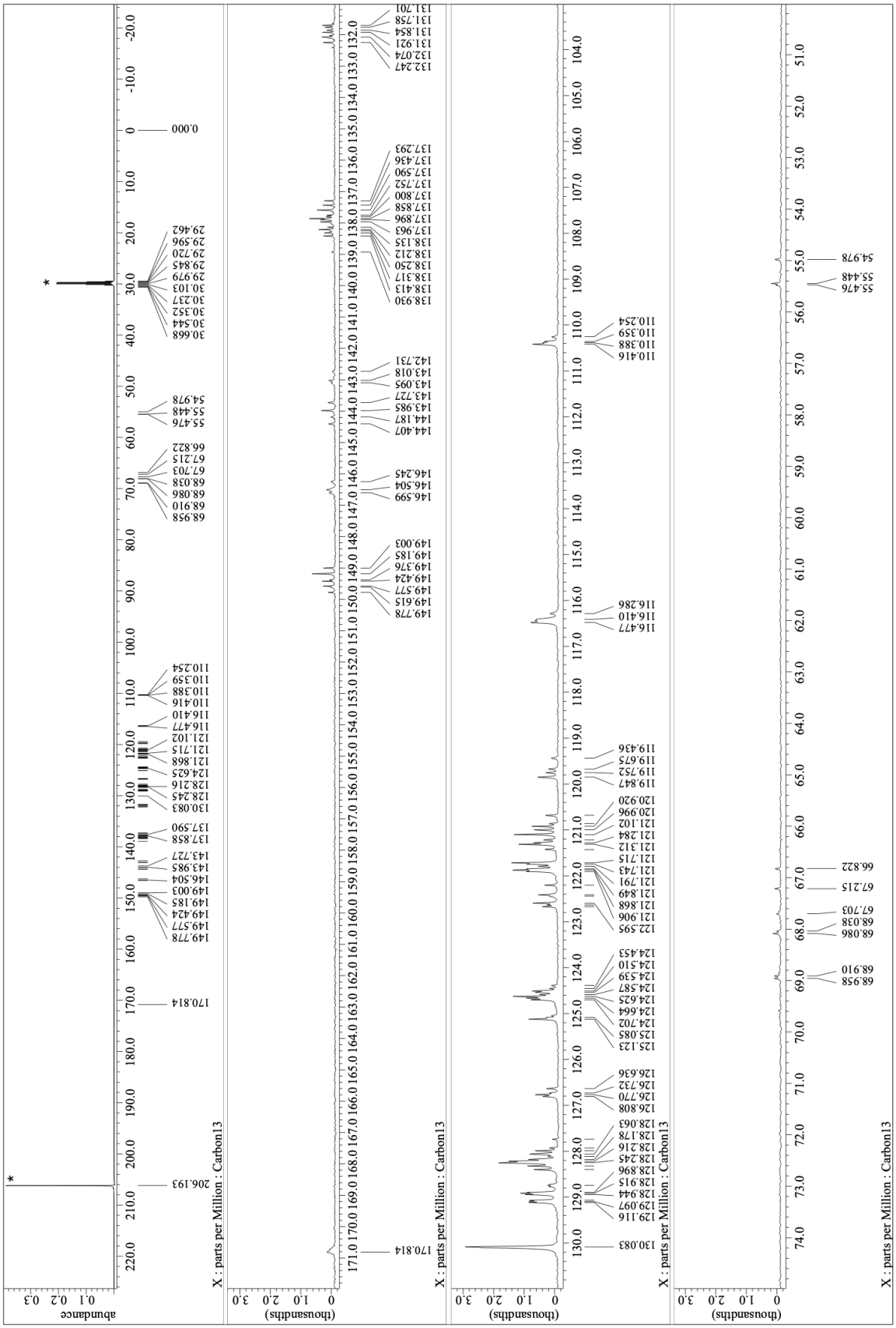

Figure S3-10. ^{13}C (151 MHz) NMR spectrum of **11a,b** in acetone-d_6 at room temperature. Peaks marked with * are due to residual solvents.

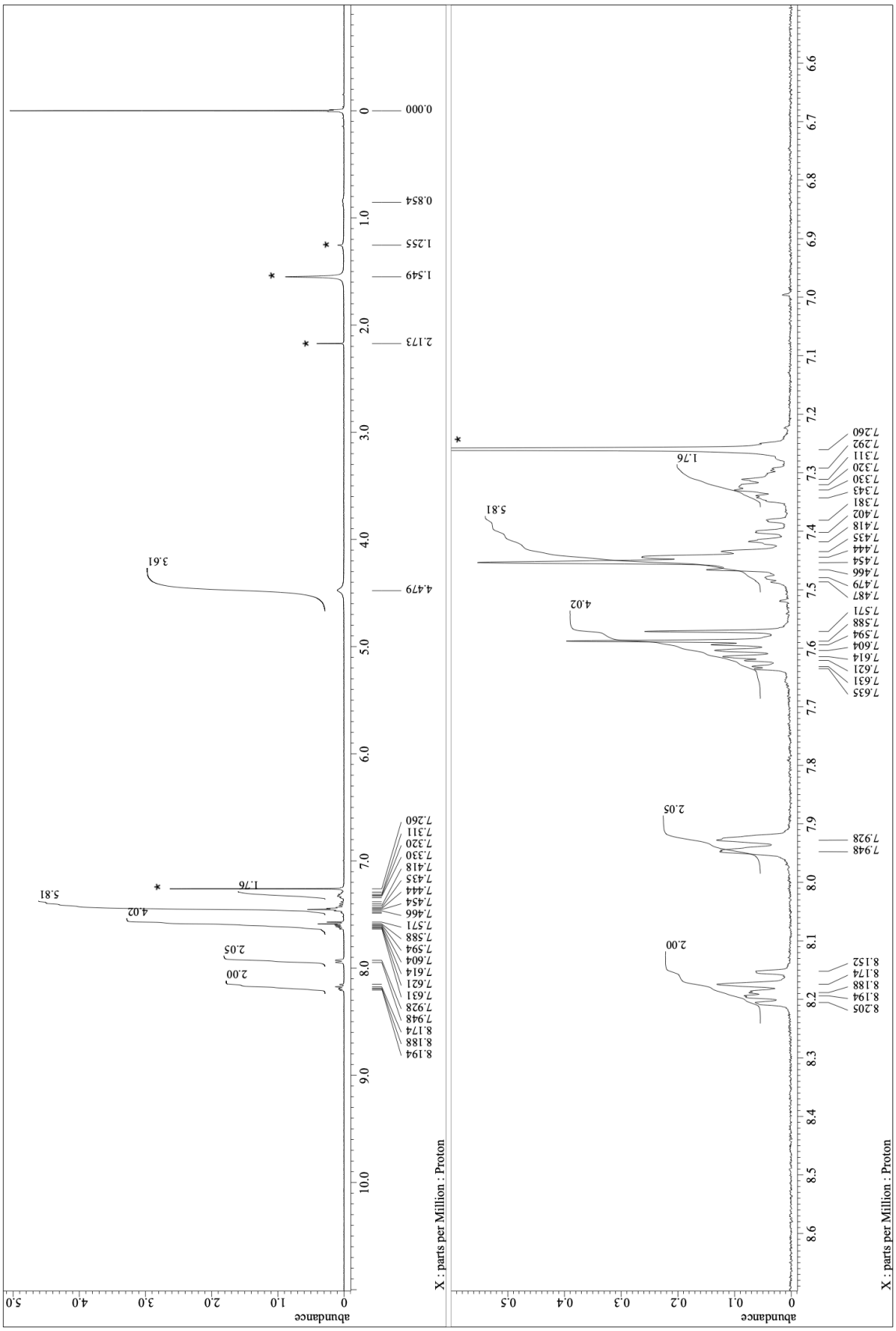

Figure S3-11. ^{1}H (400 MHz) NMR spectrum of **6a**,**b** in $CDCl_3$ at room temperature. Peaks marked with * are due to residual solvents.

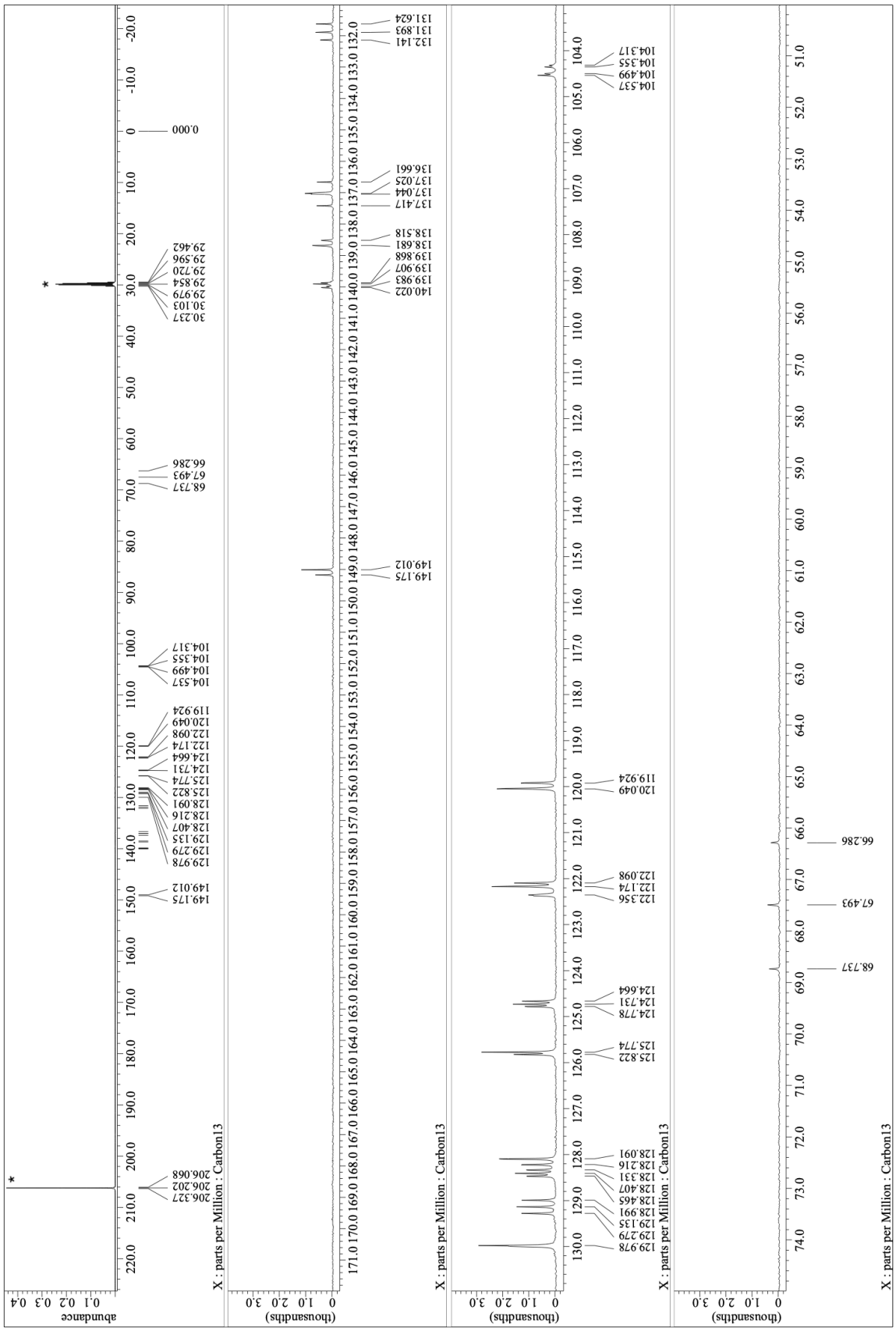

Figure S3-12. ^{13}C (151 MHz) NMR spectrum of **6a**,**b** in acetone-d_6 at room temperature. Peaks marked with * are due to residual solvents.

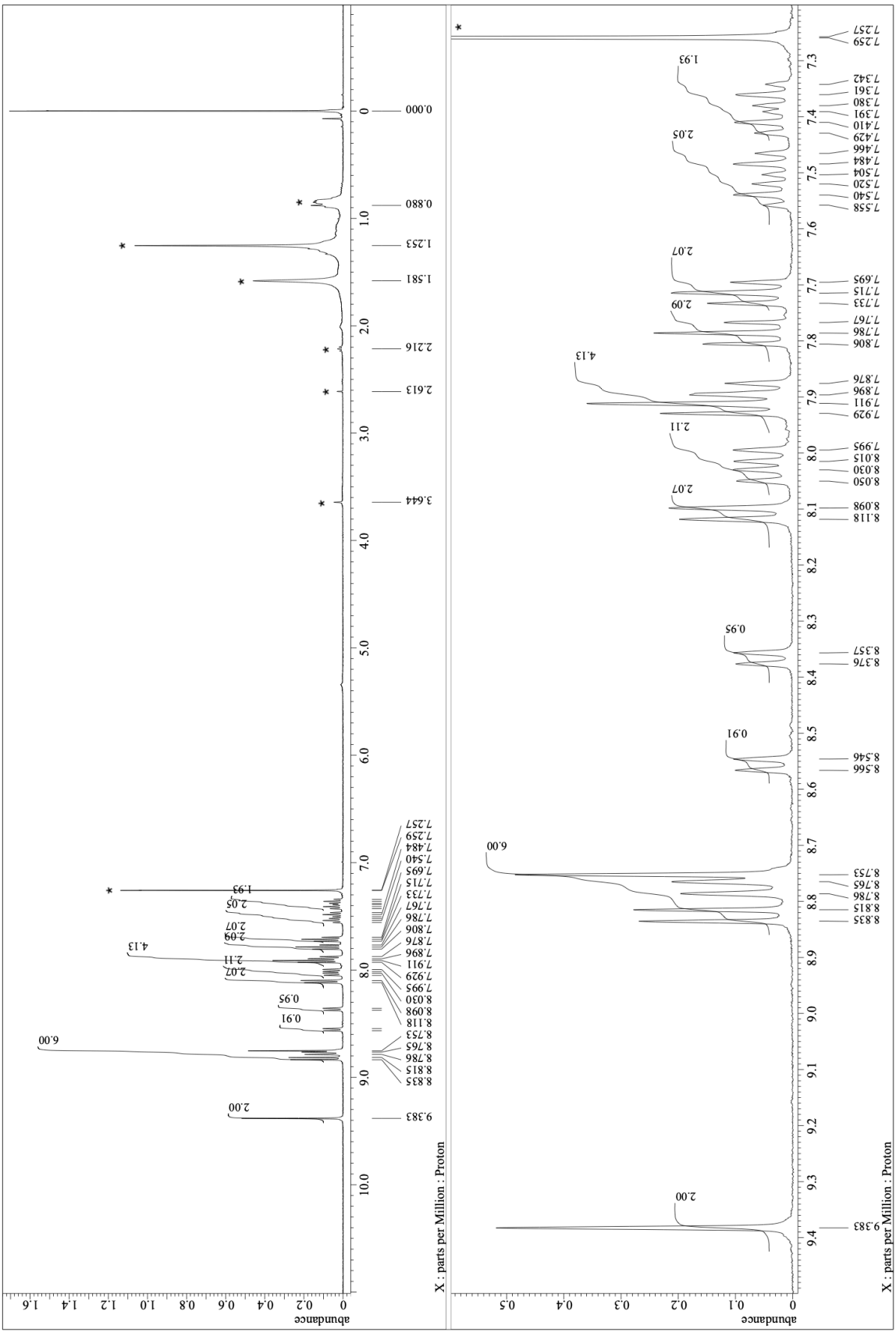

Figure S3-13. ^{1}H (400 MHz) spectra of **4a** in $CDCl_3$ at room temperature. Peaks marked with * are due to residual solvents.

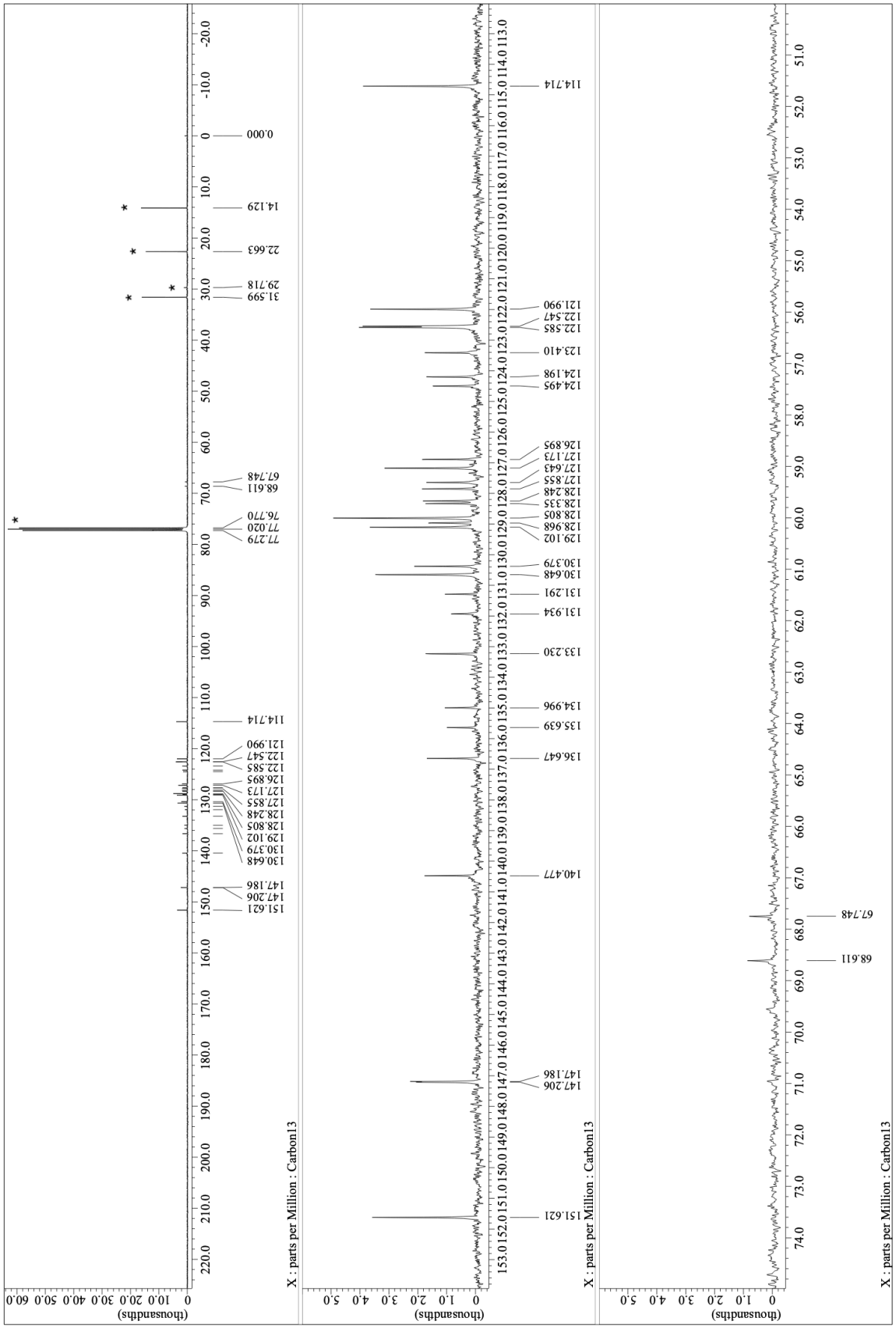

Figure S3-14. ^{13}C NMR (126 MHz) spectra of **4a** in $CDCl_3$ at room temperature. Peaks marked with * are due to residual solvents.

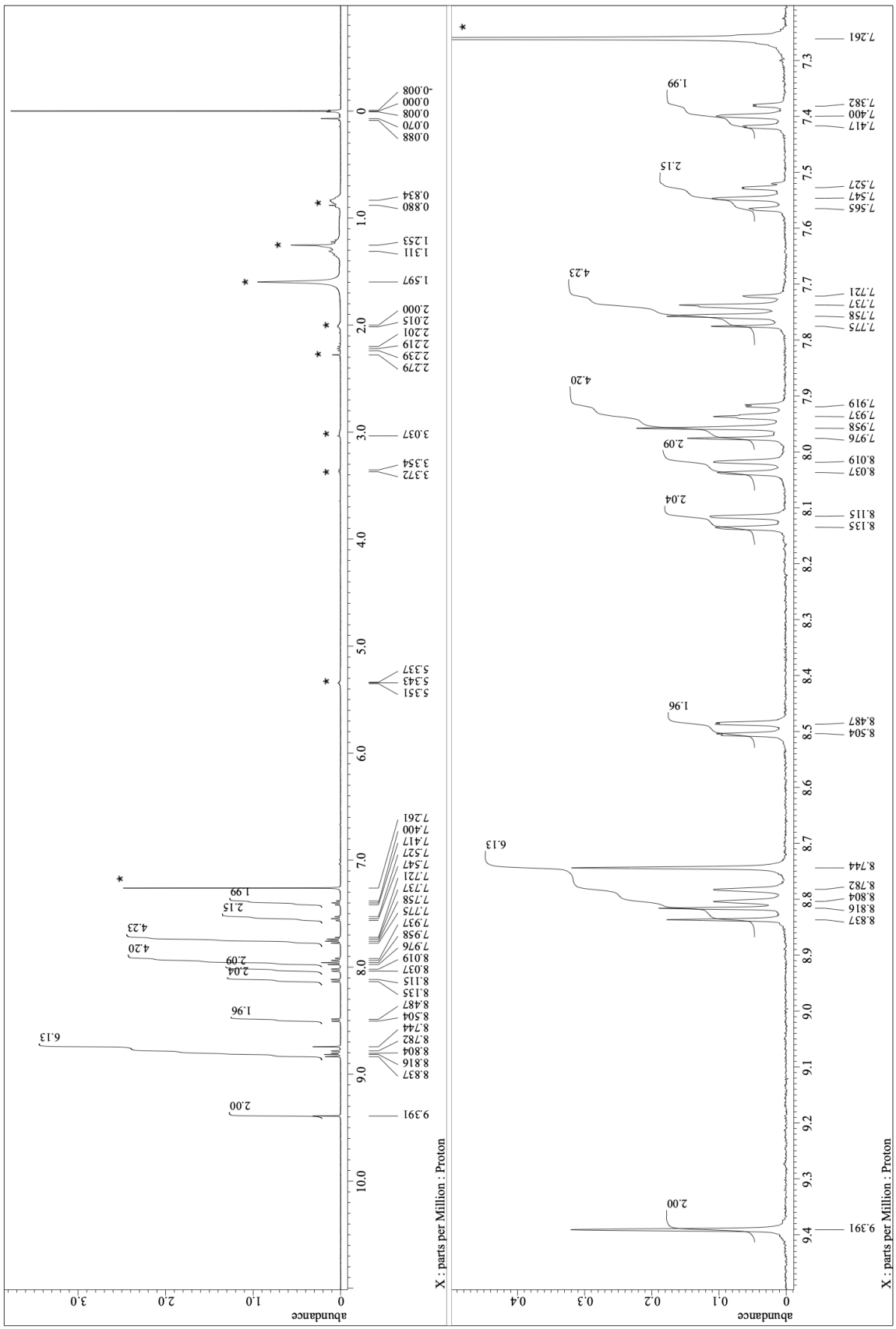

Figure S3-15. ^{1}H (400 MHz) spectra of **4b** in $CDCl_3$ at room temperature. Peaks marked with * are due to residual solvents.

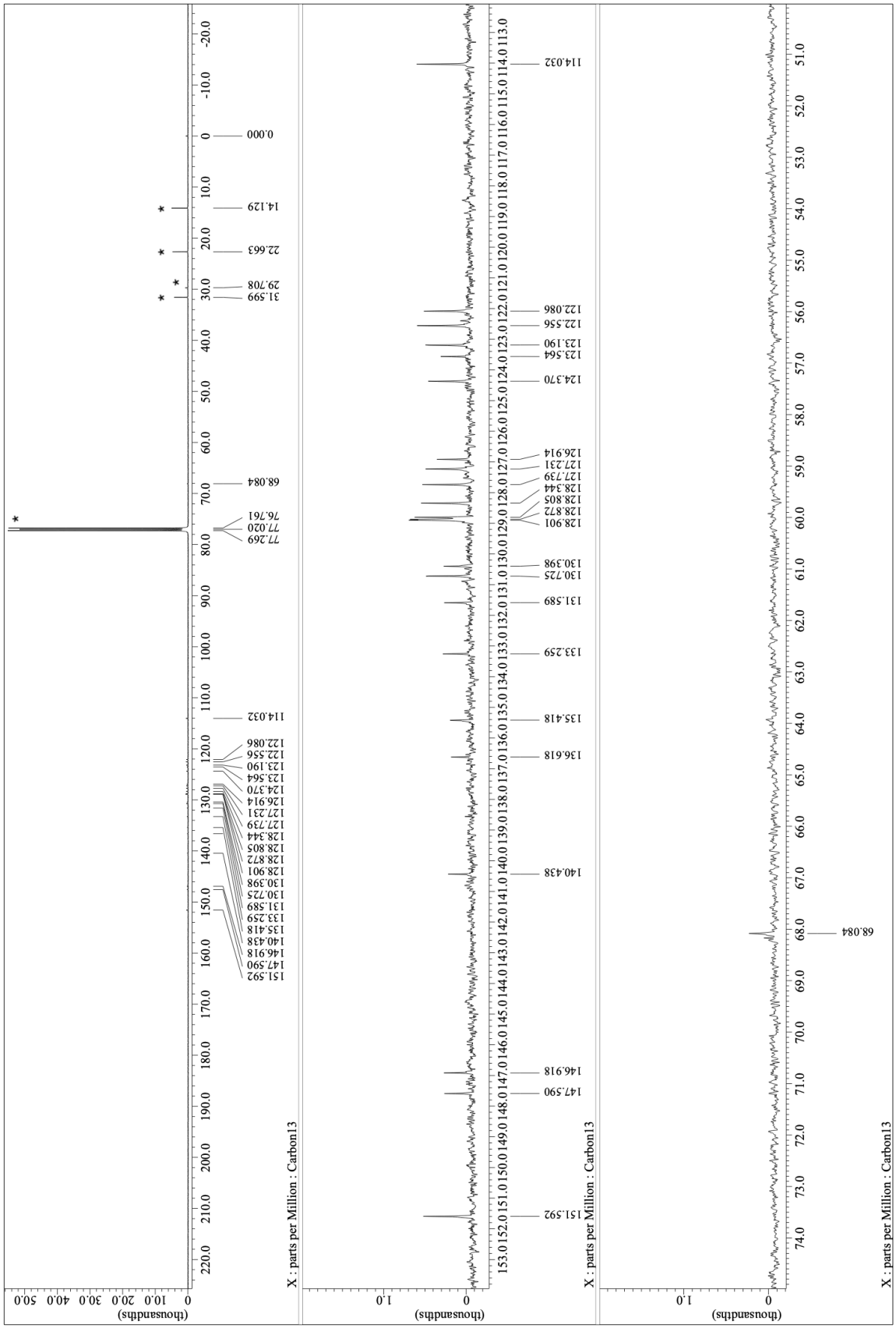

Figure S3-16. ^{13}C NMR (126 MHz) spectra of **4b** in $CDCl_3$ at room temperature. Peaks marked with * are due to residual solvents.

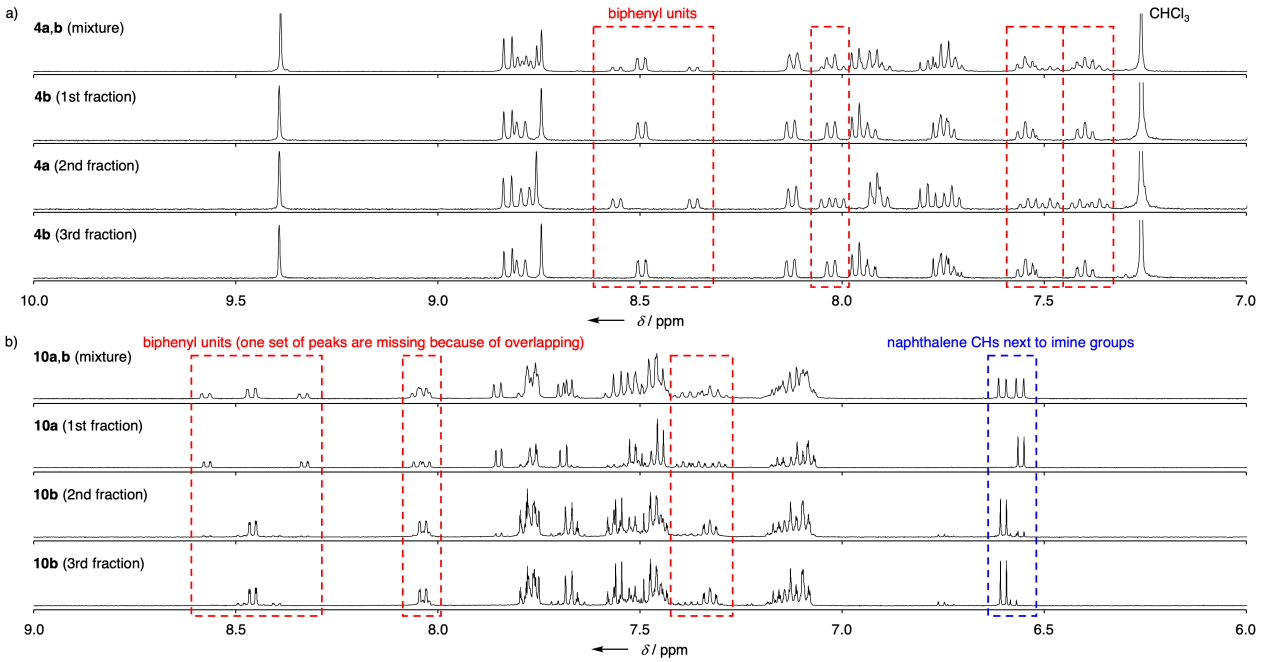

Figure S3-17. a) Comparison of ^{1}H (400 MHz) spectra of **4a**,**b** in $CDCl_3$ at room temperature. b) Comparison of ^{1}H (500 MHz) spectra of **10a**,**b** in acetone-d_6 at room temperature. Peaks marked with * are due to residual solvents.

Dibromo [4.3.3]propellane **5a**,**b** and diamino compounds **11a**,**b** and **6a**,**b** were not suitable for separation of their stereoisomers because of the low solubility in nonpolar solvents and NH-derived severe broadening upon column chromatography, respectively. On the other hand, imine **10a**,**b** was not very good for successful isolation but gave a set of fractions enriched sufficiently for ^{1}H NMR spectroscopy. The amounts of fractions were limited and therefore, peak intensities were not enough for the ^{13}C NMR spectra though overnight conditions were applied.

4. High-resolution APCI-FT-MS

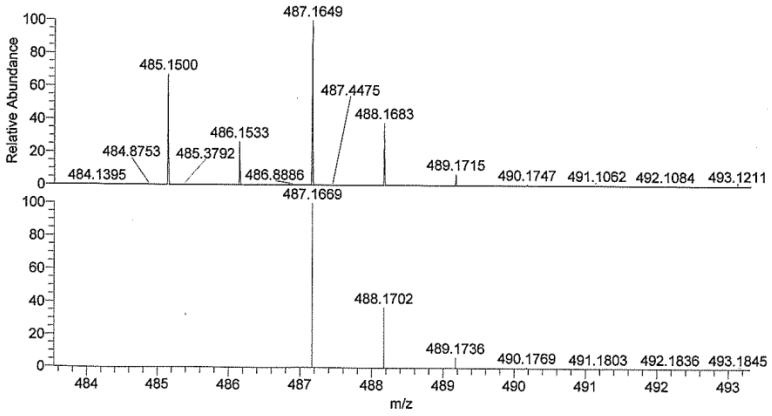

Figure S4-1. Observed (top) and simulated (bottom) high-resolution APCI-FT-MS of **9**.

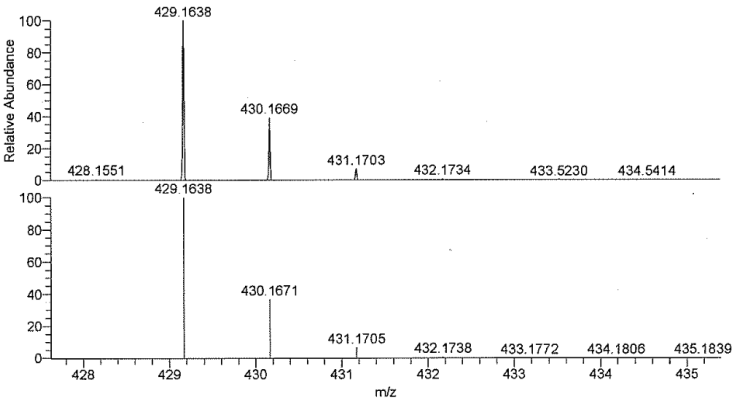

Figure S4-2. Observed (top) and simulated (bottom) high-resolution APCI-FT-MS of **3**.

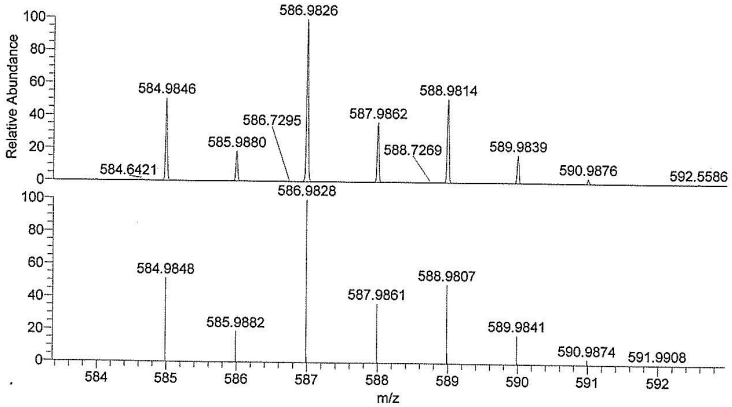

Figure S4-3. Observed (top) and simulated (bottom) high-resolution APCI-FT-MS of **5a**,**b**.

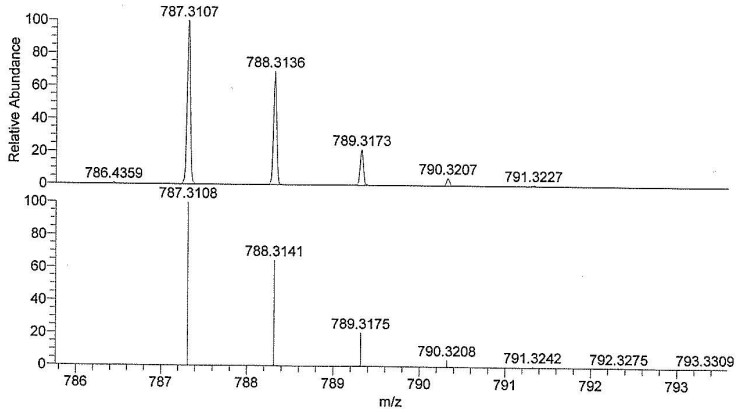

Figure S4-4. Observed (top) and simulated (bottom) high-resolution APCI-FT-MS of **10a**,**b**.

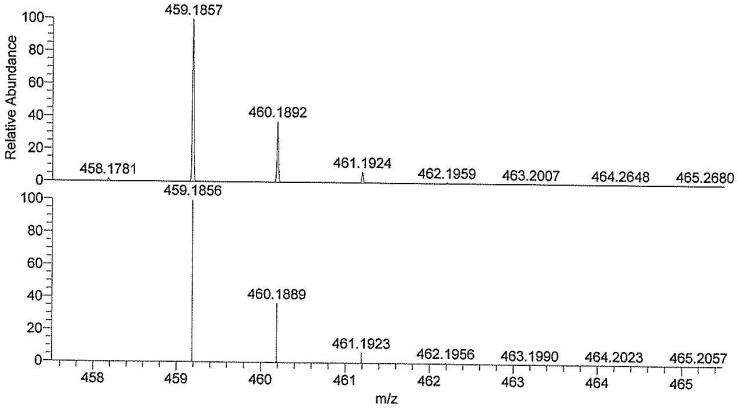

Figure S4-5. Observed (top) and simulated (bottom) high-resolution APCI-FT-MS of **11a**,**b**.

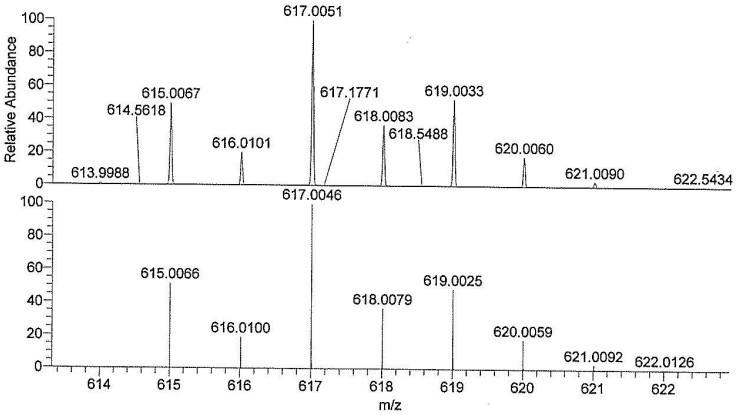

Figure S4-6. Observed (top) and simulated (bottom) high-resolution APCI-FT-MS of **6a**,**b**.

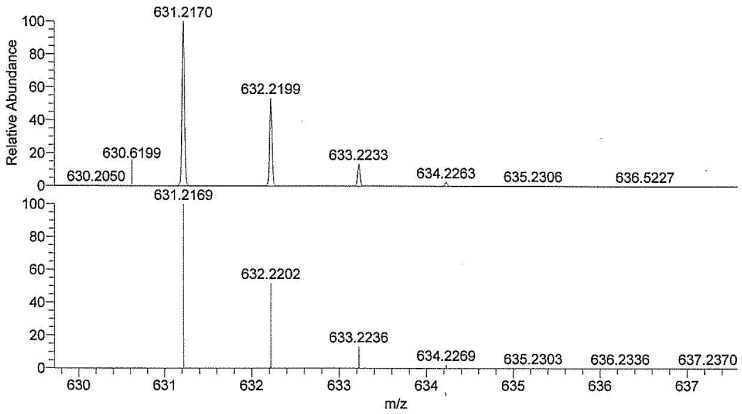

Figure S4-7. Observed (top) and simulated (bottom) high-resolution APCI-FT-MS of **4a**.

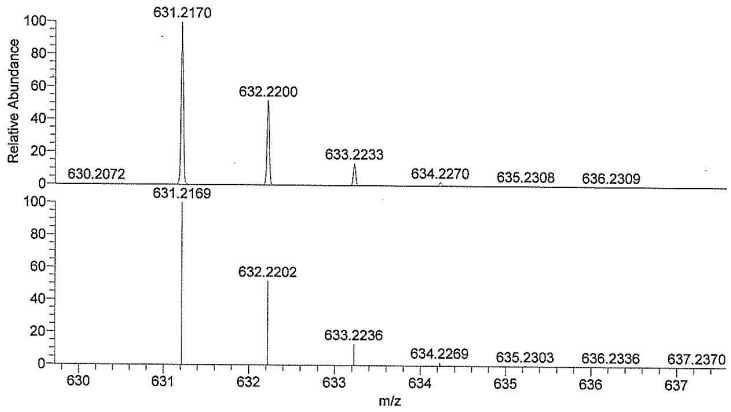

Figure S4-8. Observed (top) and simulated (bottom) high-resolution APCI-FT-MS of **4b**.

5. UV/vis Absorption and Fluorescence Spectra

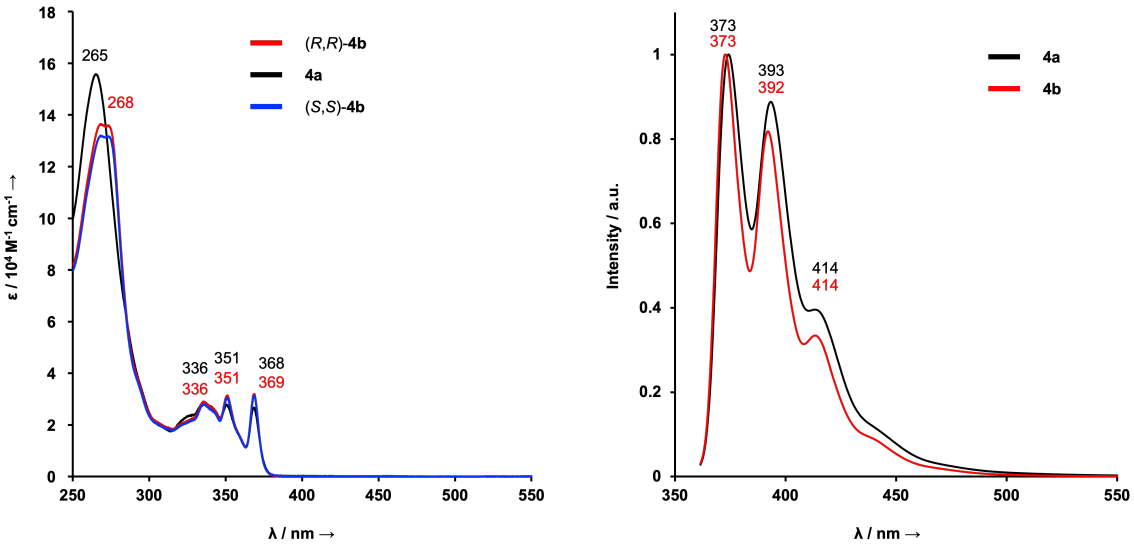

Figure S5-1. UV/vis absorption (left) and fluorescence (right) spectra of **4a**,**b** in $CHCl_3$. The excitation wavelength was set at 335 nm.

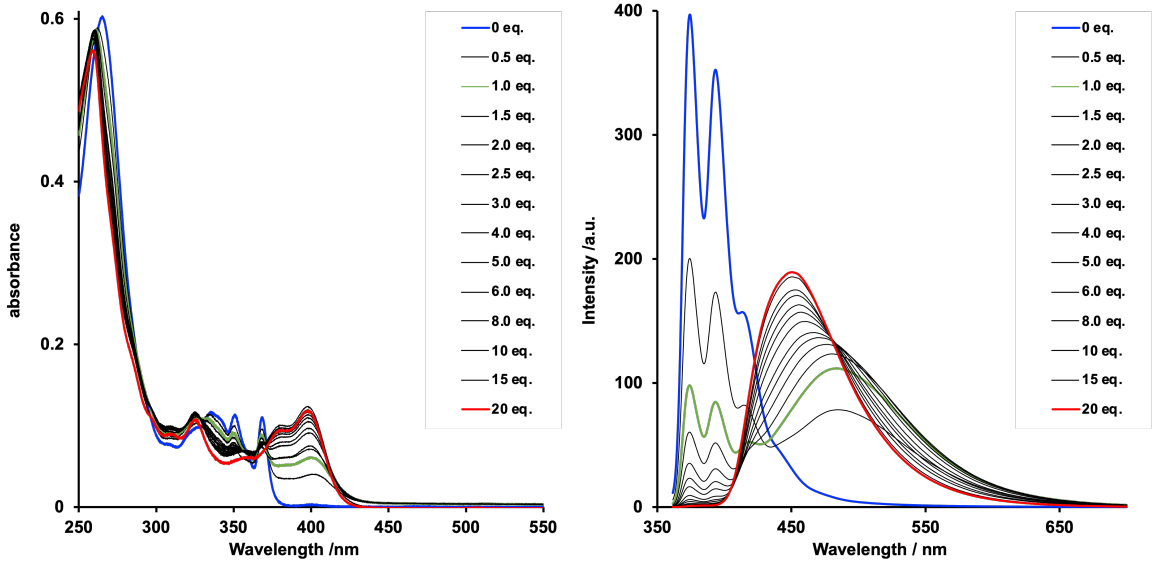

Figure S5-2. Spectral changes of UV/vis absorption (left) and fluorescence (right) spectra of **4a** in $CHCl_3$ (5.3 μM), upon addition of varying amounts of methanesulfonic acid.

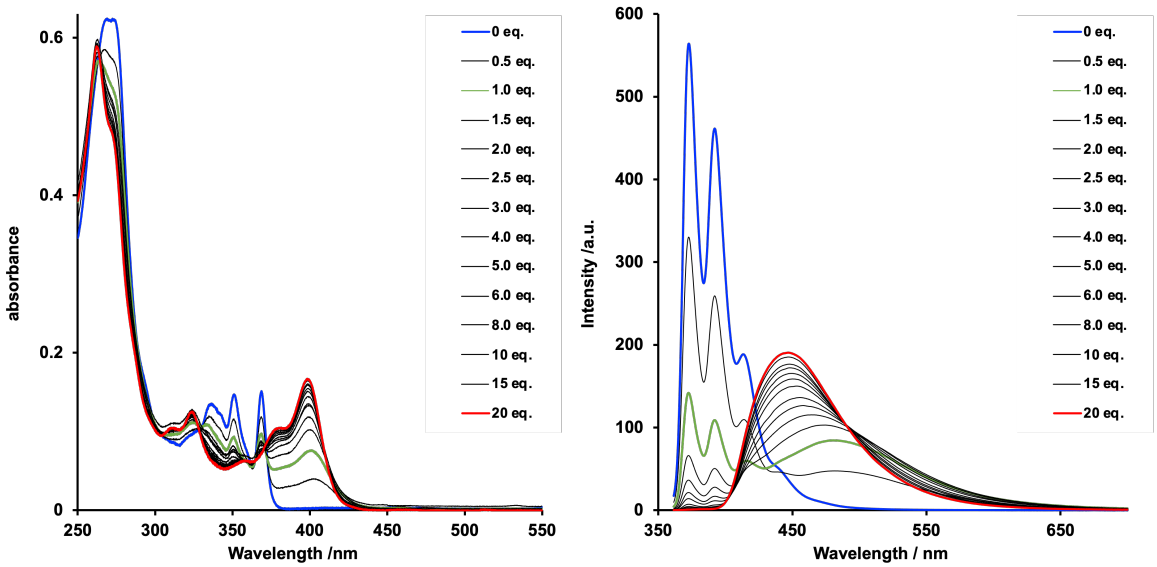

Figure S5-3. Spectral changes of UV/vis absorption (left) and fluorescence (right) spectra of **4b** in $CHCl_3$ (6.0 μM), upon addition of varying amounts of methanesulfonic acid.

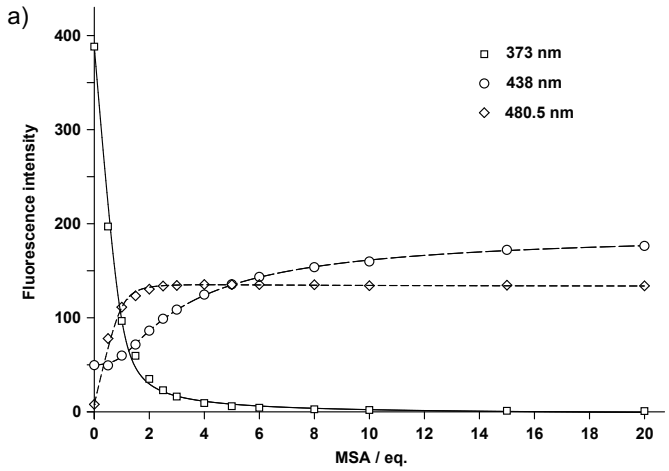

	K_1	$2.09\times10^6 \pm 5.6\times10^5$
	K_2	$4.23\times10^4 \pm 8.3\times10^3$
		Intensity
373 nm	[M]	388.2
	$[MH]^+$	19.3 ± 8.3
	$[MH_2]^{2+}$	-3.2 ± 4.1
438 nm	[M]	49.57
	$[MH]^+$	52.2 ± 5.1
	$[MH_2]^{2+}$	193 ± 6
480.5 nm	[M]	7.967
	$[MH]^+$	140 ± 4
	$[MH_2]^{2+}$	133 ± 3

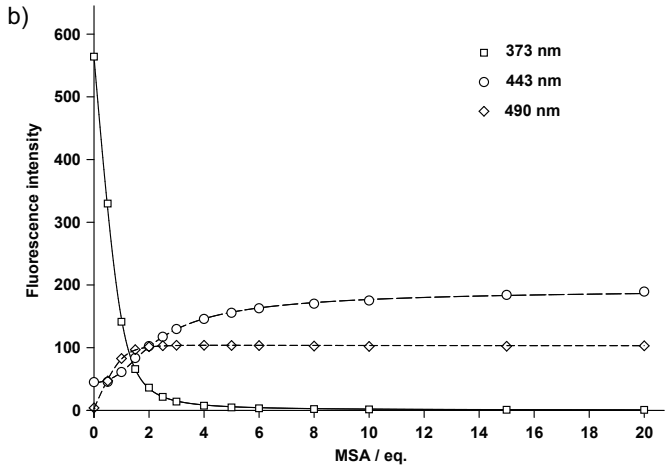

	K_1	$1.92\times10^6 \pm 1.8\times10^5$
	K_2	$8.58\times10^4 \pm 6.4\times10^3$
		Intensity
373 nm	[M]	563.9
	$[MH]^+$	18.0 ± 5.1
	$[MH_2]^{2+}$	-2.1 ± 1.4
443 nm	[M]	43.5
	$[MH]^+$	50.1 ± 2.5
	$[MH_2]^{2+}$	195 ± 2
490 nm	[M]	2.99
	$[MH]^+$	108 ± 2
	$[MH_2]^{2+}$	102 ± 1

Figure S5-4. Fluorescence intensity plots and fitting curves (left), and value tables (right, underlined values were set as constants) for the acid titration of a) **4a** and b) **4b**. The fitting curves were derived from the least squares method using 14 conditions. The three fitting wavelengths were selected from the following criteria: 1) peak top at the shortest wavelength, 2) first isosbestic point, and 3) second isosbestic point. The fitting parameters and protonation constants were obtained based on the equation below, where K_1, K_2 denoted the equilibrium constants and M stood for propellane molecules **4a** and **4b**.

$$K_1 = \frac{[\mathrm{MH^+}]}{[\mathrm{M}][\mathrm{H^+}]}$$

$$K_2 = \frac{[\mathrm{MH^{2+}}]}{[\mathrm{MH^+}][\mathrm{H^+}]}$$

6. HPLC Charts and Chiroptical Measurement

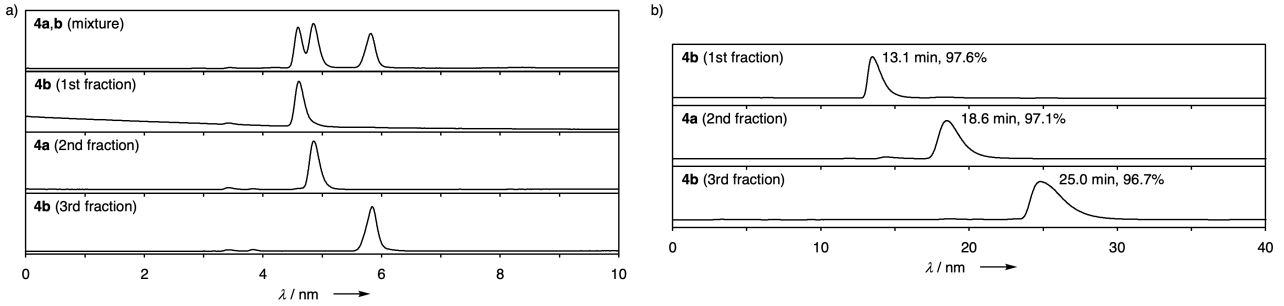

Figure S6-1. a) Preparative HPLC charts of **4a**,**b** recorded as absorption of 300 nm light. Conditions: CHIRALPAK IA (φ = 10 mm, l = 250 mm), room temperature, flow rate = 5 mL/min, eluent = $CHCl_3$/*n*-hexane/Et_3N = 1/1/0.01. b) Analytical HPLC charts of pure stereoisomers of **4a**,**b** recorded as absorption of 254 nm light. Conditions: CHIRALPAK IA (φ = 4.6 mm, l = 250 mm), room temperature, flow rate = 1.0 mL/min, eluent = $CHCl_3$/*n*-hexane = 25/75. The retention time of each peak is also shown along with the percentage of the peak area.

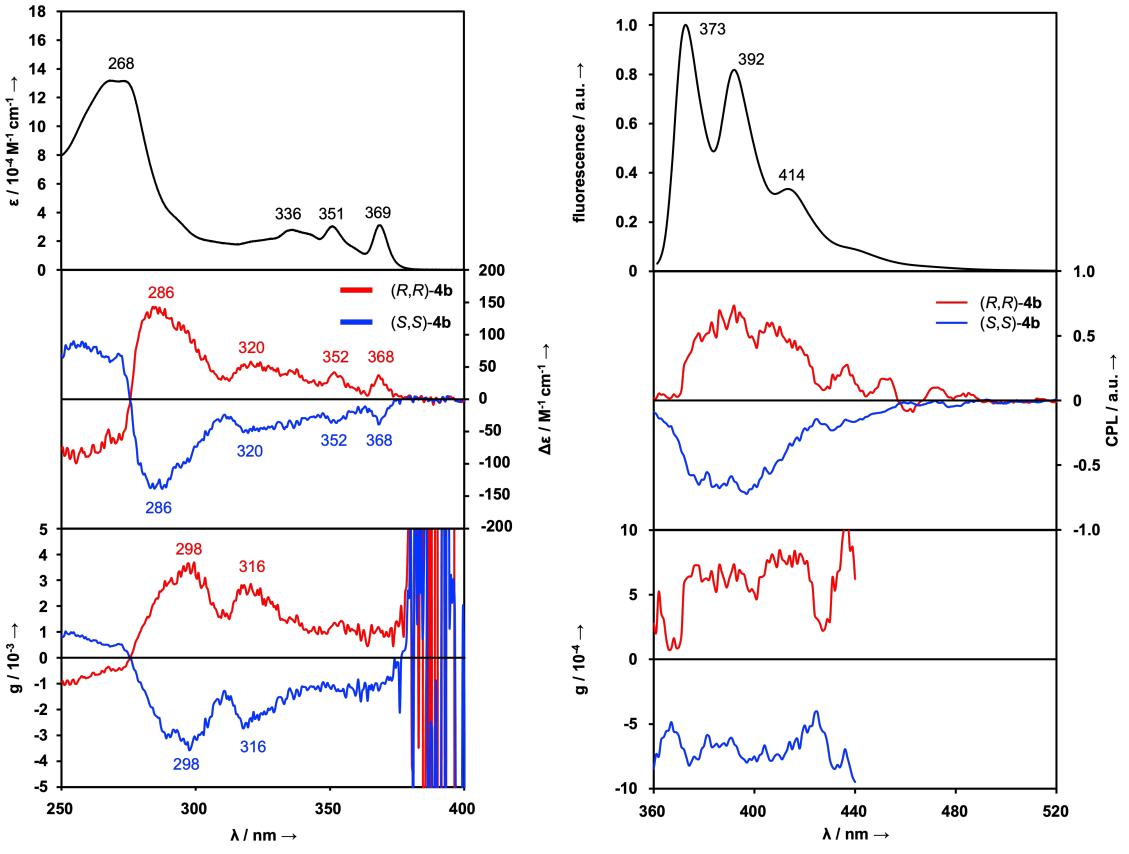

Figure S6-2. a) UV/vis absorption (top) and CD (middle) spectra in $CHCl_3$, and dissymmetry factor plots (bottom, $g_{CD} = \Delta\varepsilon/\varepsilon$) of **4b**. b) Fluorescence (top) and CPL (middle) spectra in $CHCl_3$, and dissymmetry factor plots (bottom) of **4b**. Excitation wavelengths were set at 335 and 290 nm for fluorescence and CPL measurement respectively.

7. Theoretical Calculations

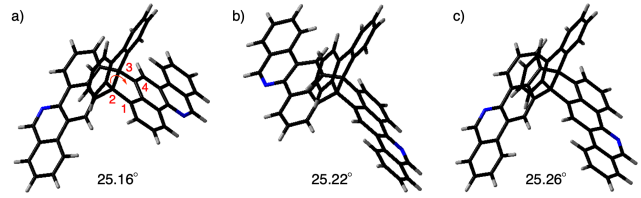

Figure S7-1. Optimized structures of a) (*R*,*R*,*P*)-**4b**, b) (*S*,*S*,*P*)-**4b**, and c) **4a** with the average of three torsion angles around the central C–C bonds.

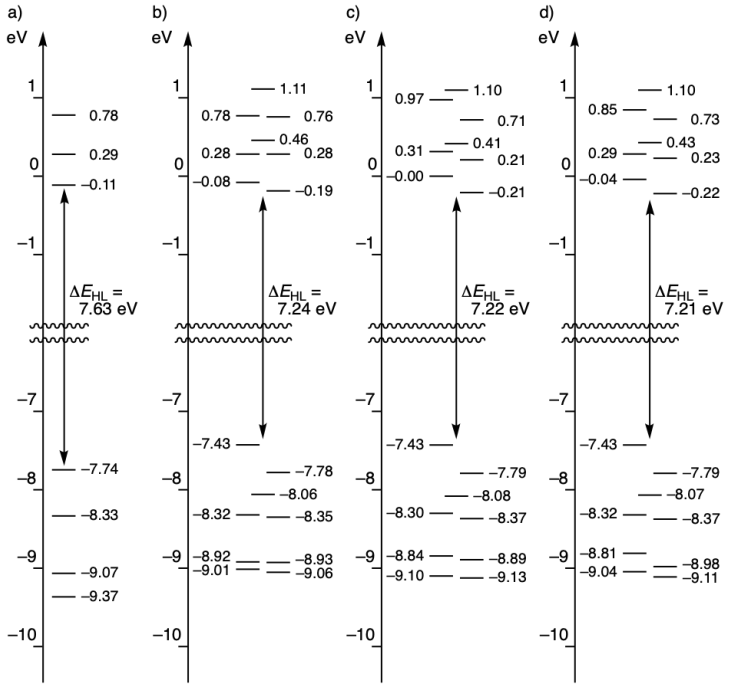

Figure S7-2. Energy diagrams of a) 5-azacrysene, b) (*R*,*R*,*P*)-**4b**, c) (*S*,*S*,*P*)-**4b**, and d) **4a**.

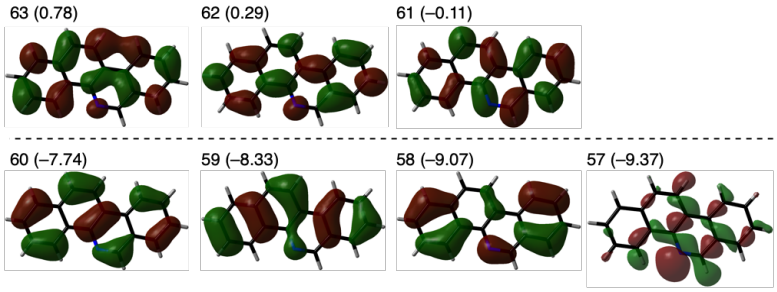

Figure S7-3. Kohn-Sham orbital representations of 5-azachrysene.

Table S7-1. Calculated parameters for electronic transitions of 5-azachrysene.

state	wavelength [nm]	oscillator strength	*R* [erg esu cm G^{-1}]	E-M angle [°]	major components
1	304.52	0.0739	-0.00×10^{-38}	90.00	60 > 62 (0.43), 60 > 61 (–0.37)
2	293.17	0.0995	-0.00×10^{-38}	90.00	60 > 61 (0.54), 59 > 61 (0.24)
3	269.45	0.0013	0.00×10^{-38}	90.00	57 > 61 (0.43), 57 > 62 (–0.15)
4	258.68	0.0214	0.00×10^{-38}	90.00	60 > 63 (0.43), 59 > 62 (–0.29)
5	245.03	1.0715	-0.00×10^{-38}	90.00	59 > 61 (0.49), 60 > 62 (–0.41)
6	240.77	0.2169	0.00×10^{-38}	90.00	60 > 63 (0.44), 58 > 61 (0.30)
7	230.54	0.2271	-0.00×10^{-38}	90.00	59 > 62 (0.43), 59 > 63 (–0.25)
8	230.51	0.0005	0.00×10^{-38}	90.00	57 > 62 (0.64), 57 > 63 (0.18)
9	223.66	0.4285	-0.00×10^{-38}	90.00	58 > 61 (0.57), 60 > 63 (–0.24)
10	208.00	0.0554	-0.00×10^{-38}	90.00	59 > 63 (0.46), 58 > 62 (–0.45)

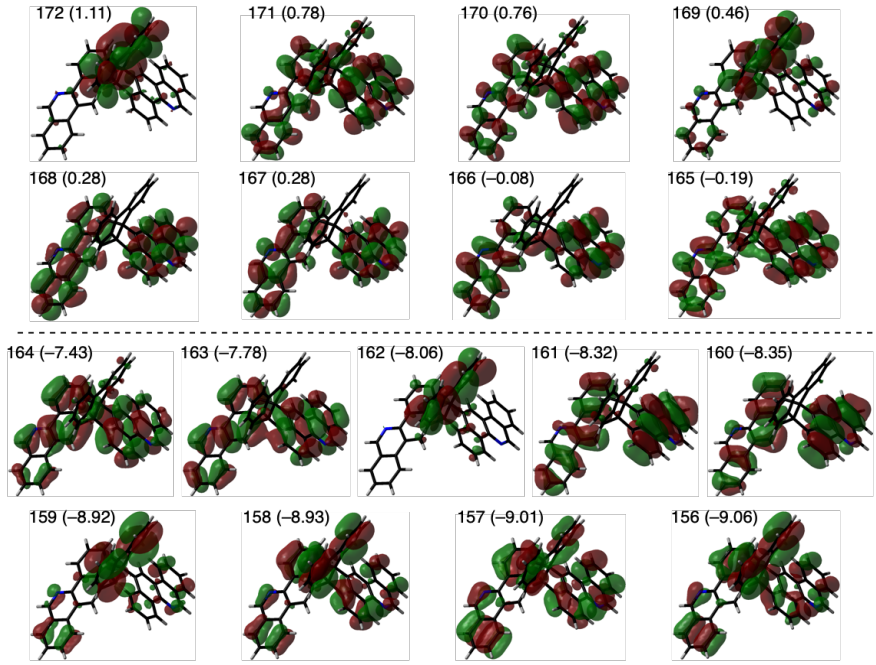

Figure S7-4. Kohn-Sham orbital representations of (*R*,*R*,*P*)-**4b**.

Table S7-2. Calculated parameters for selected electronic transitions of (*R*,*R*,*P*)-**4b**.

state	wavelength [nm]	oscillator strength	*R* [erg esu cm G^{-1}]	E-M angle [°]	major components
1	310.98	0.4482	1.46×10^{-38}	73.06	164 > 165 (0.50), 163 > 166 (–0.39)
2	310.33	0.0967	-1.49×10^{-38}	90.00	164 > 166 (0.37), 164 > 168 (–0.29)
4	298.37	0.1082	0.58×10^{-38}	90.00	163 > 165 (0.36), 164 > 166 (–0.35)
9	262.94	0.0373	-1.68×10^{-38}	149.71	164 > 171 (0.35), 163 > 170 (–0.31)
10	255.60	0.0874	2.43×10^{-38}	8.81	161 > 167 (0.26), 162 > 172 (0.25)
11	254.31	0.2257	-11.49×10^{-38}	90.00	160 > 165 (0.31), 164 > 166 (–0.31)
12	251.81	0.0805	-0.84×10^{-38}	113.07	162 > 172 (0.37), 159 > 169 (0.27)
13	248.36	1.3521	14.63×10^{-38}	15.53	161 > 165 (0.36), 164 > 167 (0.35)
14	247.02	0.0525	-1.12×10^{-38}	90.00	164 > 170 (0.34), 161 > 170 (–0.20)
15	244.97	0.0703	-2.38×10^{-38}	90.00	156 > 169 (0.28), 158 > 169 (0.26)
16	240.40	0.1511	-6.22×10^{-38}	90.00	163 > 165 (0.34), 160 > 165 (0.26)
17	239.41	0.5082	4.95×10^{-38}	21.23	163 > 166 (0.36), 163 > 170 (0.29)
19	233.69	0.1871	-1.60×10^{-38}	169.45	160 > 170 (0.23), 160 > 166 (0.230
20	233.65	0.3320	0.51×10^{-38}	1.47	161 > 168 (0.32), 160 > 167 (0.28)

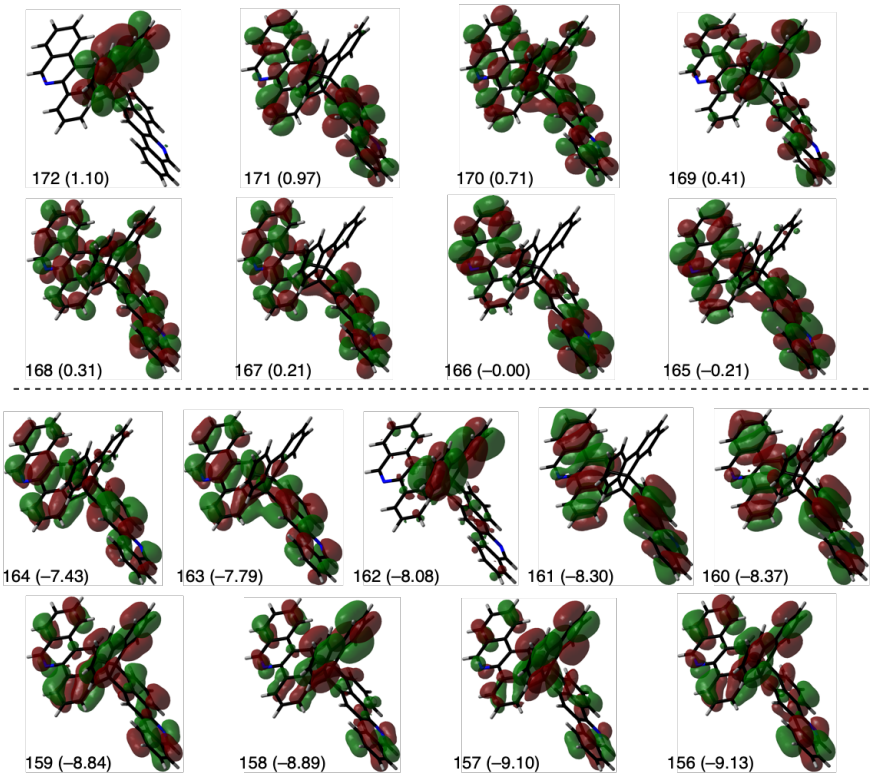

Figure S7-5. Kohn-Sham orbital representations of (*S*,*S*,*P*)-**4b**.

Table S7-3. Calculated parameters for selected electronic transitions of (*S*,*S*,*P*)-**4b**.

state	wavelength [nm]	oscillator strength	*R* [erg esu cm G^{-1}]	E-M angle [°]	major components
1	313.96	0.5838	–1.71×10^{-38}	169.14	164 > 165 (0.52), 163 > 166 (0.26)
3	303.74	0.0850	0.26×10^{-38}	67.57	164 > 168 (0.34), 163 > 167 (0.29)
4	299.29	0.0793	–0.89×10^{-38}	90.00	164 > 166 (0.47), 163 > 165 (0.42)
5	268.66	0.0394	–0.98×10^{-38}	107.41	164 > 169 (0.38), 162 > 169 (–0.26)
8	263.43	0.0895	–3.07×10^{-38}	158.30	162 > 169 (0.31), 164 > 170 (–0.31)
10	253.28	0.0293	–1.82×10^{-38}	175.76	162 > 172 (0.44), 158 > 169 (–0.25)
11	252.05	0.0154	–3.83×10^{-38}	179.82	161 > 165 (0.40), 164 > 167 (–0.36)
12	250.00	0.6142	0.90×10^{-38}	60.95	161 > 167 (0.34), 160 > 168 (–0.29)
13	249.24	1.5817	3.33×10^{-38}	80.38	161 > 166 (0.35), 164 > 168 (–0.35)
14	249.16	0.0402	–0.89×10^{-38}	2.49	163 > 169 (0.22), 163 > 170 (–0.21)
17	236.79	0.1746	-0.66×10^{-38}	106.50	162 > 165 (0.33), 164 > 169 (–0.30)
18	244.97	0.2644	3.91×10^{-38}	6.68	160 > 165 (0.26), 161 > 167 (0.25)
19	240.40	0.2392	–1.48×10^{-38}	138.27	163 > 166 (0.30), 163 > 171 (0.27)
20	232.38	0.1774	0.27×10^{-38}	0.35	160 > 167 (0.29), 161 > 168 (–0.27)

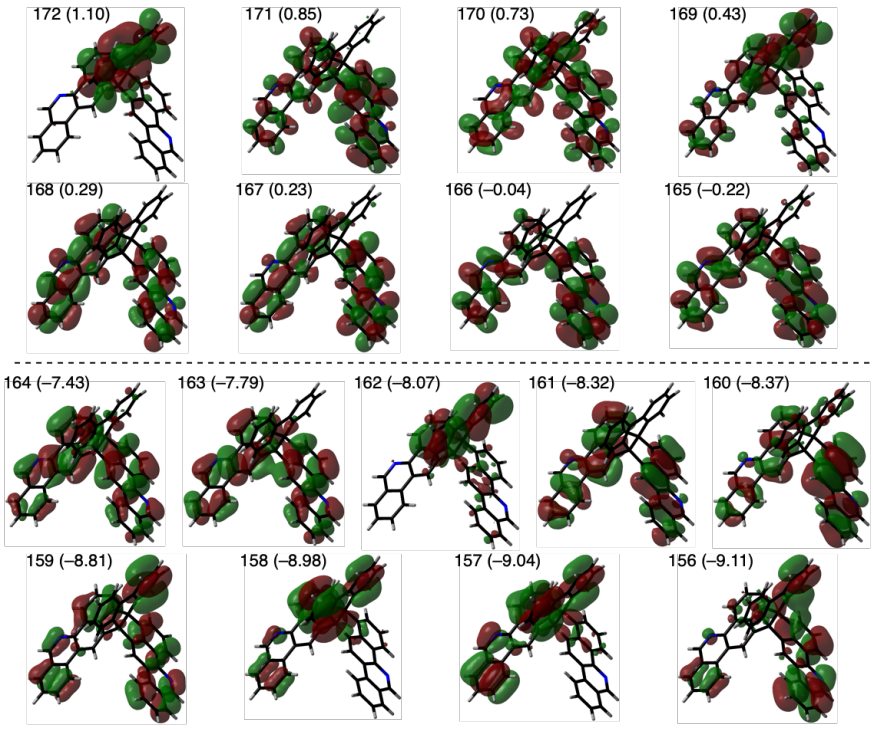

Figure S7-6. Kohn-Sham orbital representations of (*P*)-**4a**.

Table S7-4. Calculated parameters for selected electronic transitions of (*P*)-**4a**.

state	wavelength [nm]	oscillator strength	*R* [erg esu cm G^{-1}]	E-M angle [°]	major components
1	314.52	0.3425	–1.53×10^{-38}	104.07	164 > 165 (0.52), 163 > 166 (0.27)
4	298.75	0.1237	–0.20×10^{-38}	146.98	164 > 166 (0.42), 163 > 165 (0.38)
8	264.07	0.0572	-2.60×10^{-38}	133.40	164 > 170 (0.32), 162 > 169 (0.31)
10	255.50	0.2726	–7.79×10^{-38}	119.46	161 > 165 (0.30), 161 > 167 (–0.27)
11	253.51	0.0175	–0.97×10^{-38}	127.32	162 > 172 (0.39), 158 > 169 (0.23)
12	251.54	0.0694	–1.07×10^{-38}	151.09	164 > 170 (0.24), 162 > 172 (–0.22)
13	248.79	0.6038	2.87×10^{-38}	69.39	164 > 168 (0.27), 161 > 166 (0.27)
15	244.12	0.8921	6.05×10^{-38}	56.51	161 > 168 (0.21), 160 > 167 (–0.21)
16	241.52	0.2035	1.05×10^{-38}	77.85	163 > 165 (0.31), 164 > 166 (–0.24)
17	237.82	0.1992	–1.28×10^{-38}	106.01	163 > 166 (0.32), 163 > 171 (0.26)
19	235.35	0.3289	–0.40×10^{-38}	101.09	161 > 167 (0.25), 160 > 168 (–0.22)
20	232.47	0.2213	0.63×10^{-38}	66.83	160 > 167 (0.25), 161 > 168 (–0.25)

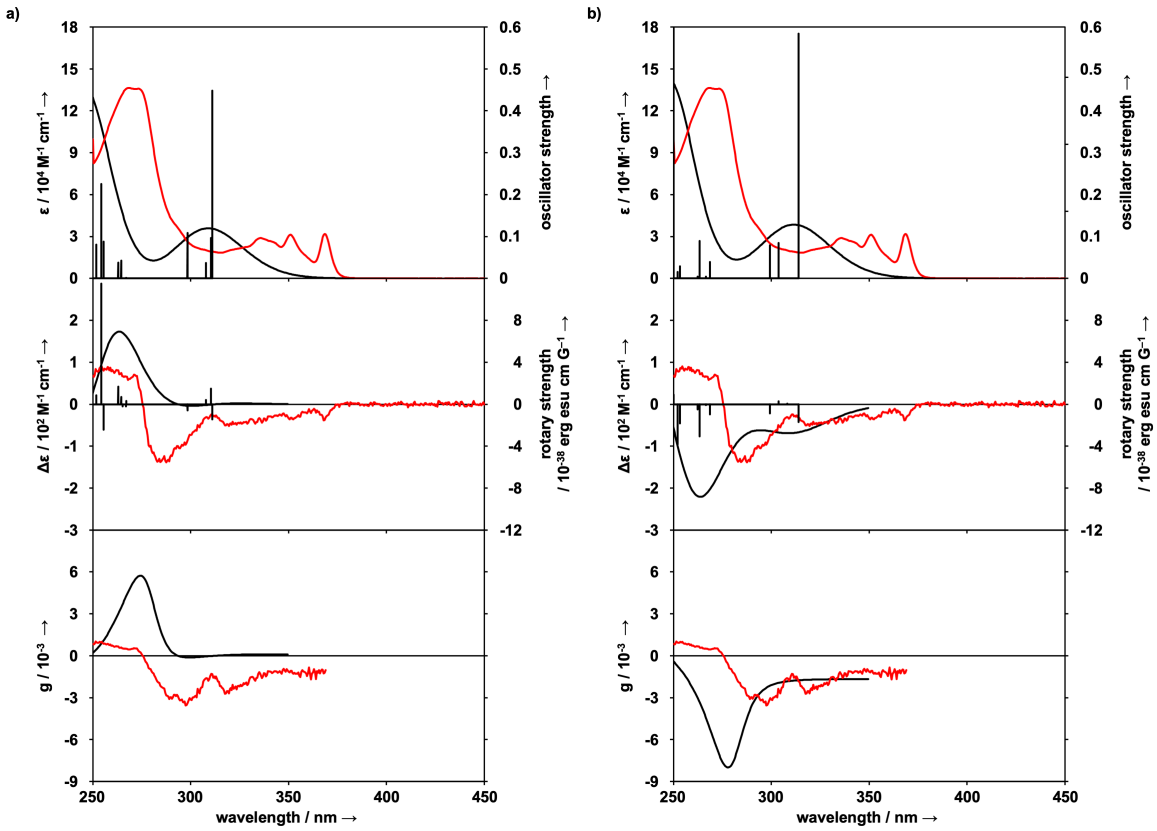

Figure S7-7. Comparison of experimental spectra of 3rd fraction of **4b** in $CHCl_3$ (red lines) and theoretical spectra of a) (*S,S,M*)-**4b** and b) (*S,S,P*)-**4b** at the TD-SCF/RωB97X-D/6-31+G(d) level (black line). UV/vis absorption (top) and CD (middle) spectra, and the resulting g_{CD} values (bottom). From this result, 1st fraction of **4b** was assigned to be (*R,R*)-enantiomer, and 3rd fraction was (*S,S*)-enantiomer. Calculated oscillator strengths and rotatory strengths are also depicted with black vertical lines. Theoretical spectra are gained by setting half width at half height at 0.25 eV.

8. References

[S1] Gaussian 16, Revision C.01, M. J. Frisch, G. W. Trucks, H. B. Schlegel, G. E. Scuseria, M. A. Robb, J. R. Cheeseman, G. Scalmani, V. Barone, G. A. Petersson, H. Nakatsuji, X. Li, M. Caricato, A. V. Marenich, J. Bloino, B. G. Janesko, R. Gomperts, B. Mennucci, H. P. Hratchian, J. V. Ortiz, A. F. Izmaylov, J. L. Sonnenberg, D. Williams-Young, F. Ding, F. Lipparini, F. Egidi, J. Goings, B. Peng, A. Petrone, T. Henderson, D. Ranasinghe, V. G. Zakrzewski, J. Gao, N. Rega, G. Zheng, W. Liang, M. Hada, M. Ehara, K. Toyota, R. Fukuda, J. Hasegawa, M. Ishida, T. Nakajima, Y. Honda, O. Kitao, H. Nakai, T. Vreven, K. Throssell, J. A. Montgomery, Jr., J. E. Peralta, F. Ogliaro, M. J. Bearpark, J. J. Heyd, E. N. Brothers, K. N. Kudin, V. N. Staroverov, T. A. Keith, R. Kobayashi, J. Normand, K. Raghavachari, A. P. Rendell, J. C. Burant, S. S. Iyengar, J. Tomasi, M. Cossi, J. M. Millam, M. Klene, C. Adamo, R. Cammi, J. W. Ochterski, R. L. Martin, K. Morokuma, O. Farkas, J. B. Foresman and D. J. Fox, Gaussian, Inc., Wallingford CT, 2019.

[S2] B3LYP, Becke's three-parameter hybrid exchange functionals and the Lee–Yang–Parr correction functional: a) A. D. Becke, *J. Chem. Phys*., 1993, **98**, 1372–1377; b) C. Lee, W. Yang, R. G. Parr, *Phys. Rev. B*, 1988, **37**, 785–789.

[S3] ϖB97X-D, long-range corrected (LC) hybrid density functional including empirical atom–atom dispersion corrections: J.-D. Chai, M. Head-Gordon, *Phys. Chem. Chem. Phys*., 2008, **10**, 6615–6620.